



**The Abdus Salam
International Centre for Theoretical Physics**



2328-12

**Preparatory School to the Winter College on Optics and the Winter College on
Optics: Advances in Nano-Optics and Plasmonics**

30 January - 17 February, 2012

Optical antennas: Intro and basics

J. Aizpurua

*Center for Materials Physics, CSIC-UPV/EHU and Donostia International Physics
Center - DIPIC
Spain*

Optical antennas: Intro and basics

Javier Aizpurua



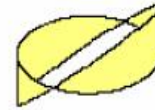
<http://cfm.ehu.es/nanophotonics>

*Center for Materials Physics, CSIC-UPV/EHU
and Donostia International Physics Center - DIPC
Donostia-San Sebastián, the Basque Country, Spain*

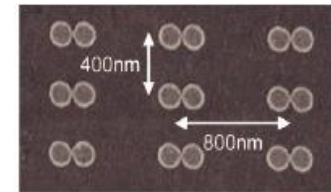
***Winter College on Optics: Advances in Nano-Optics and Plasmonics
February 6-17, 2012
The Abdus Salam International Centre for Theoretical Physics, Trieste, Italy***

Outline

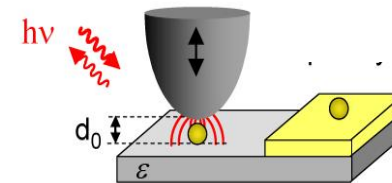
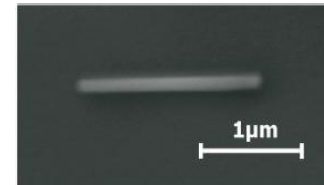
- Optical antennas: Basics



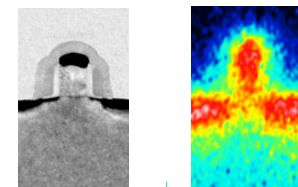
- Playing with modes



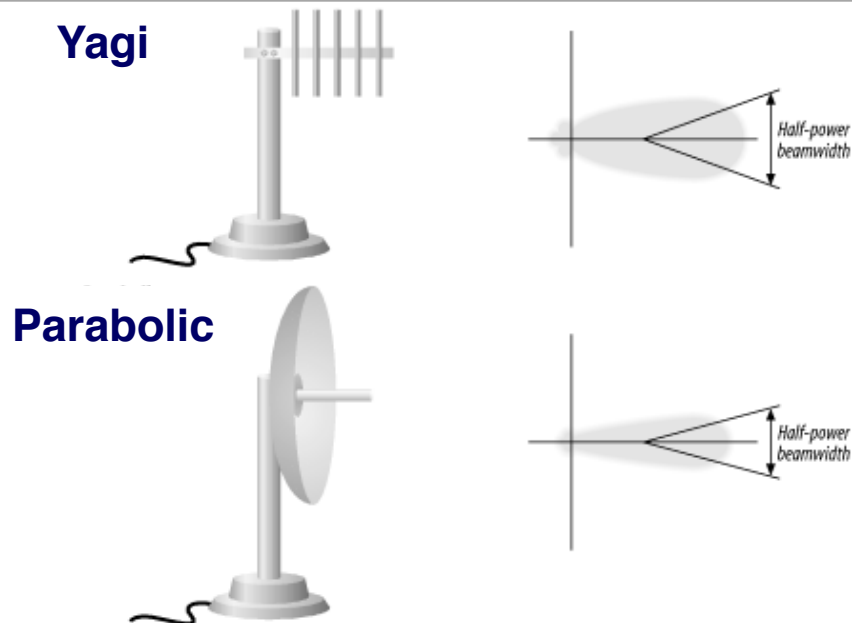
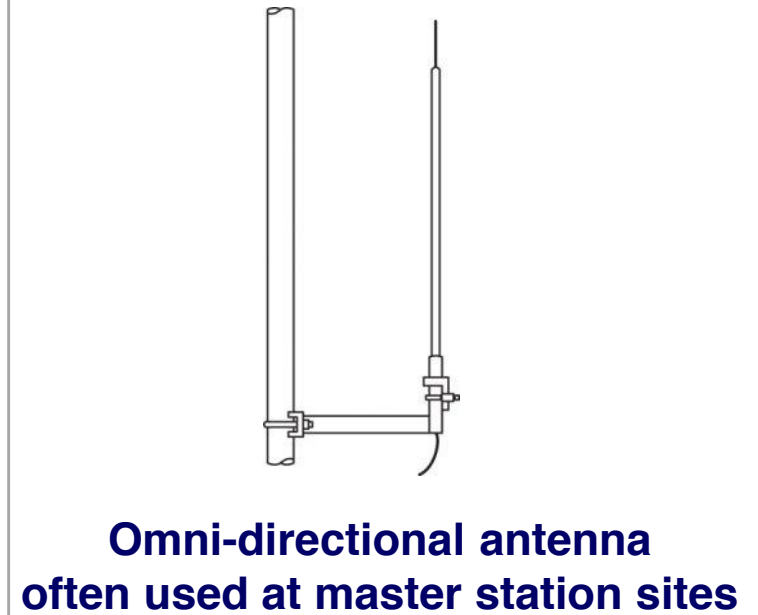
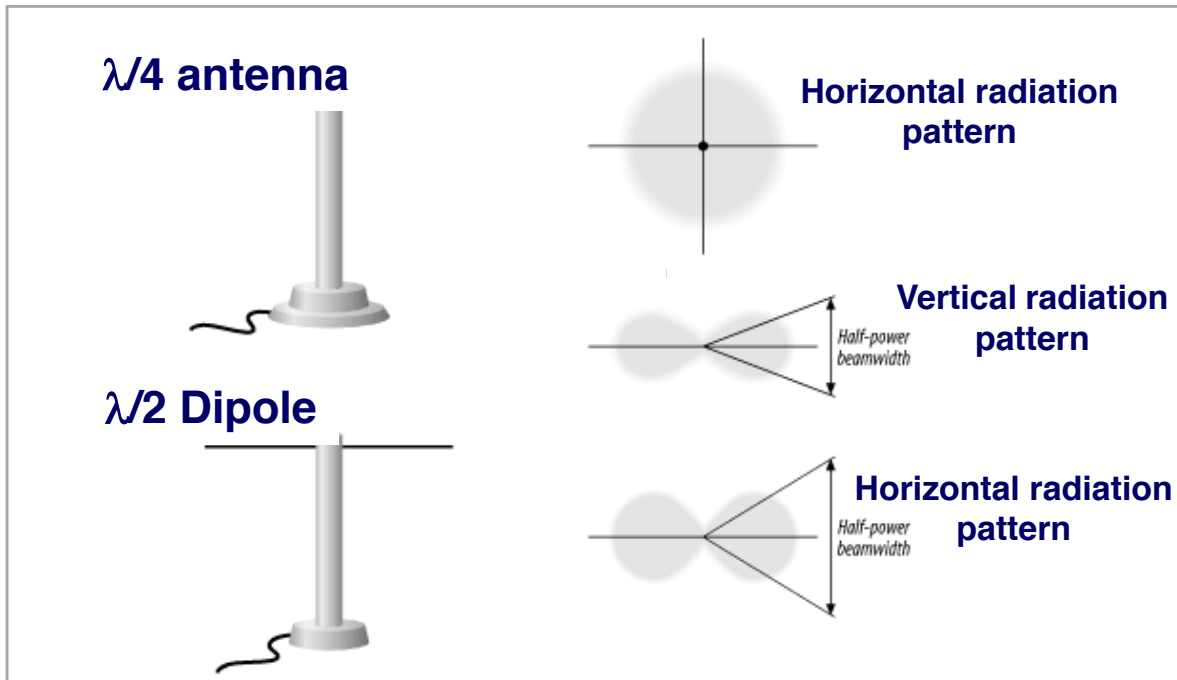
- Optical antennas for Enhanced Spectroscopy: SERS and SEIRA



- More applications of Optical antennas



Different types of radio antennas



Radio Frequency Antennas



Half wave dipole antennas



Biconical antenna



Monopole antenna



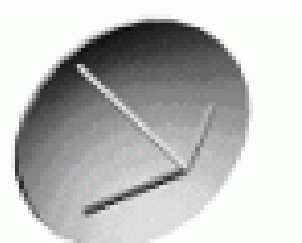
Comilog antenna



Yagi-Uda antenna



Horn antenna

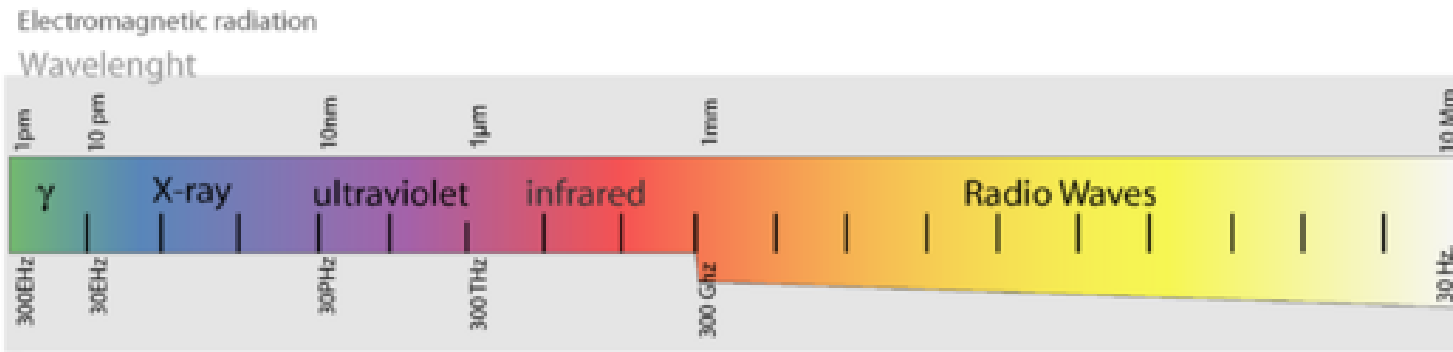


Parabolic antenna

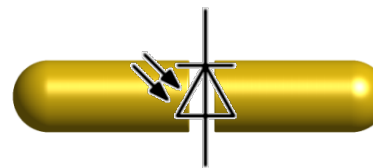
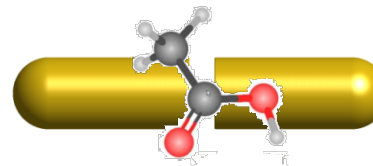
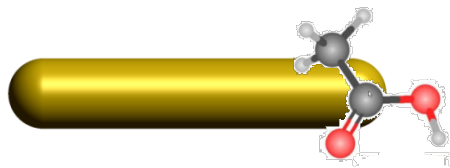
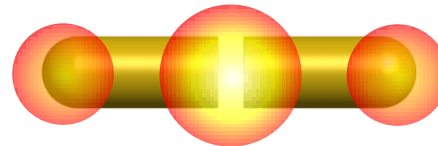


Active loop antenna

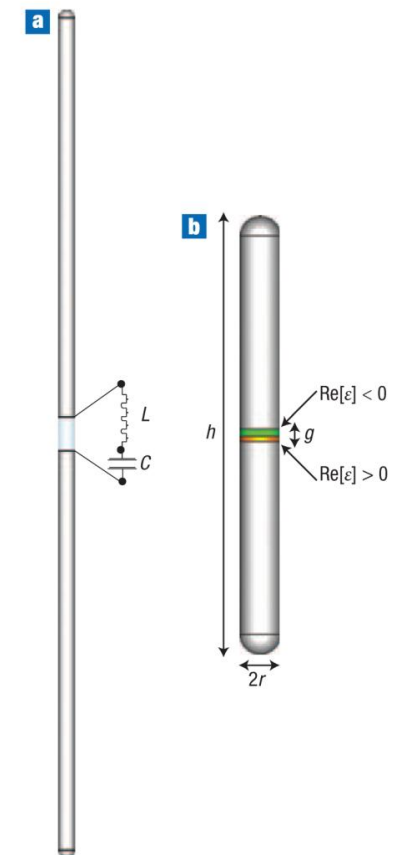
Scaling down in size ← Scaling down in wavelength



Visible light \leftrightarrow Optical antenna \leftrightarrow Nanoantenna

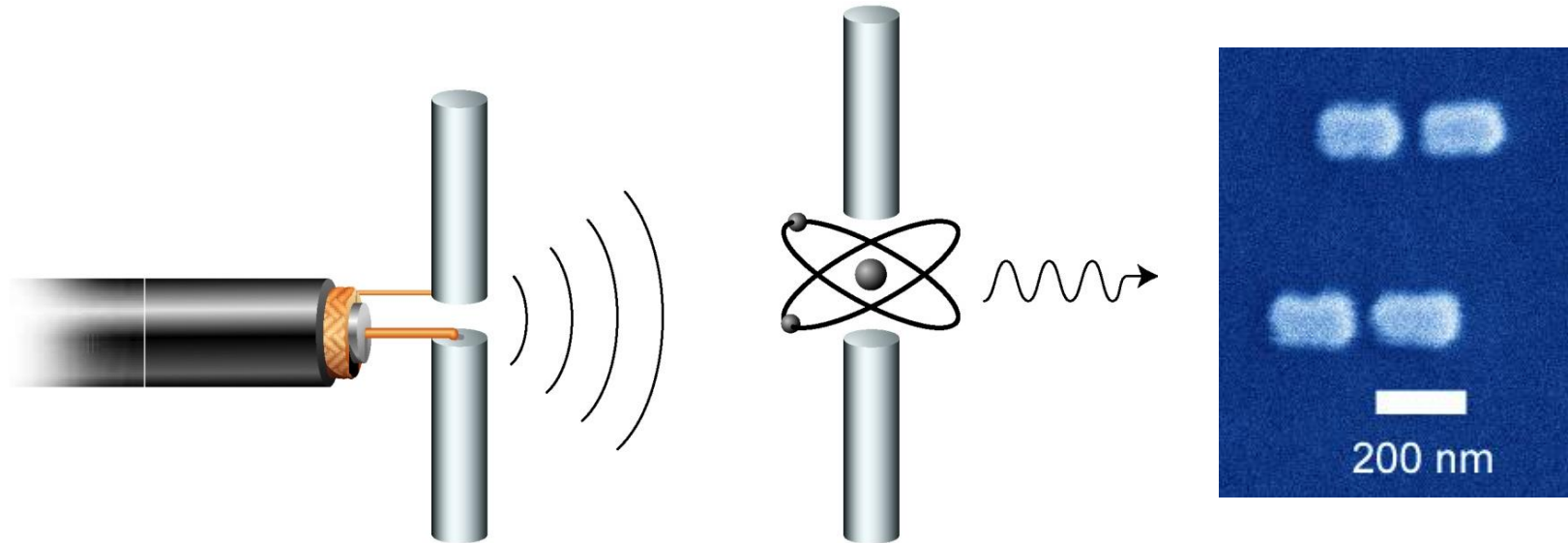


$\lambda/2$ nanoantenna



Optical nanoantennas

- Design of plasmonic nanoparticles: size, shape, interactions, ...

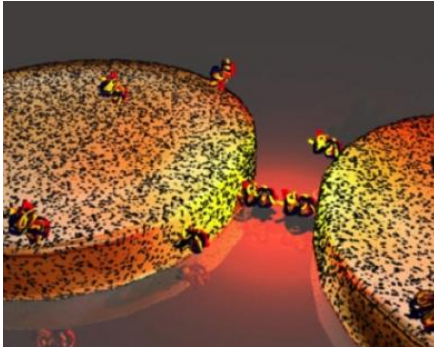


Analogy with radio-wave antennas

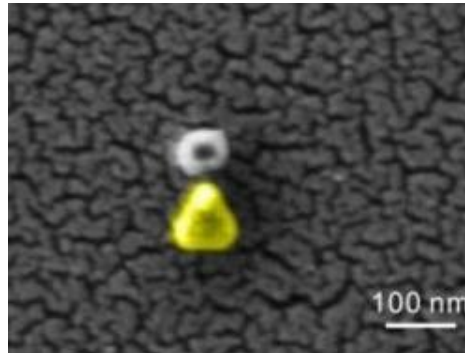
Mühschlegel et al. Science 308, 1607 (2005)

Optical nanoantennas

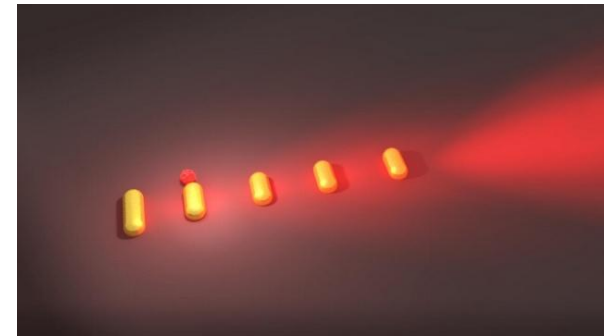
- Applications: biosensing, nonlinear optics / SERS, fluorescence, quantum optics,...



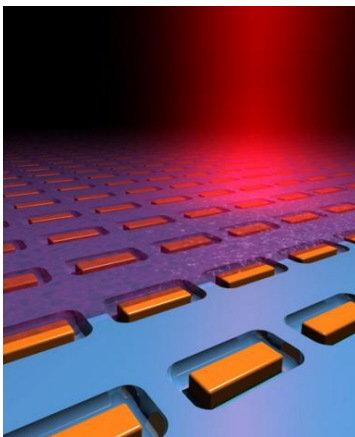
Quidant, ICFO
Antenna-gap sensing



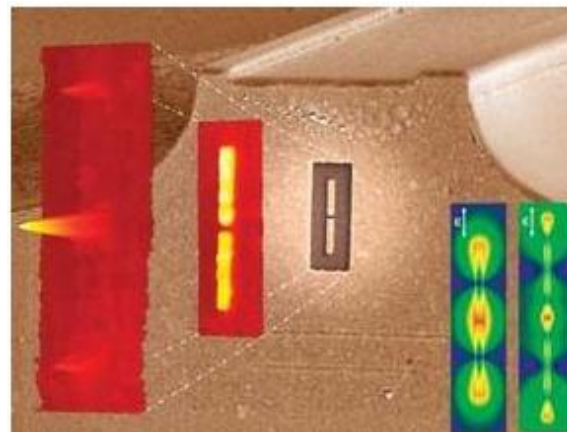
Alivisatos, Giessen
Pd-antenna sensor



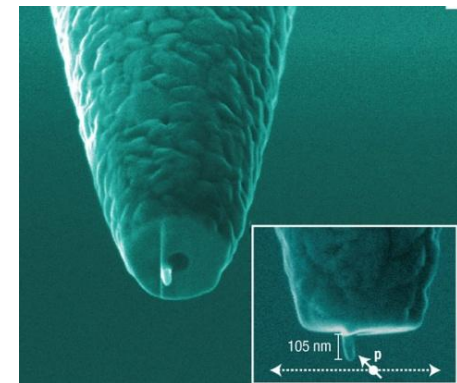
Van Hulst, ICFO - Single molecule, scanning probe



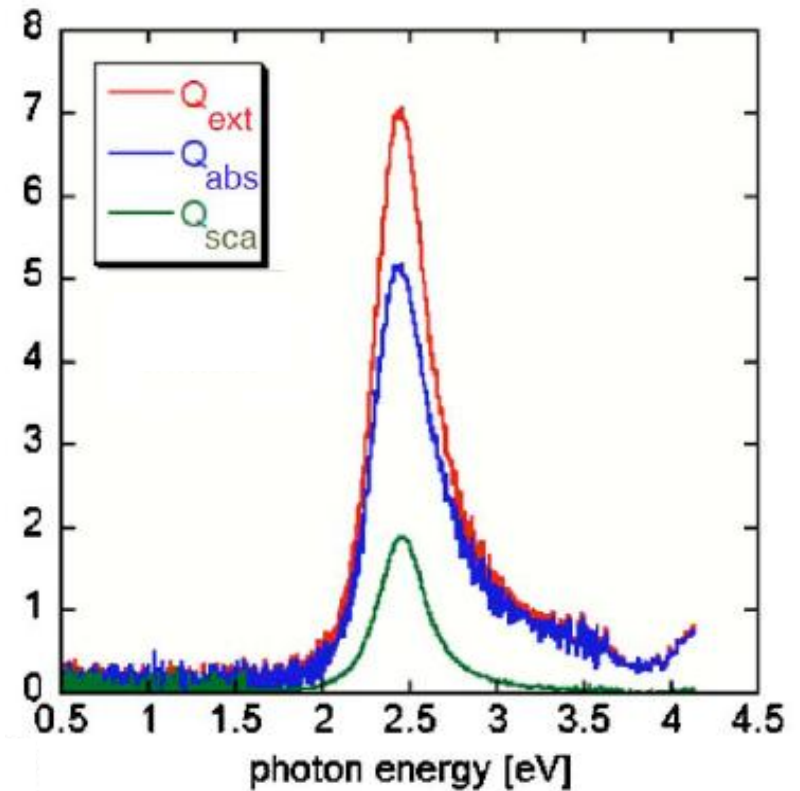
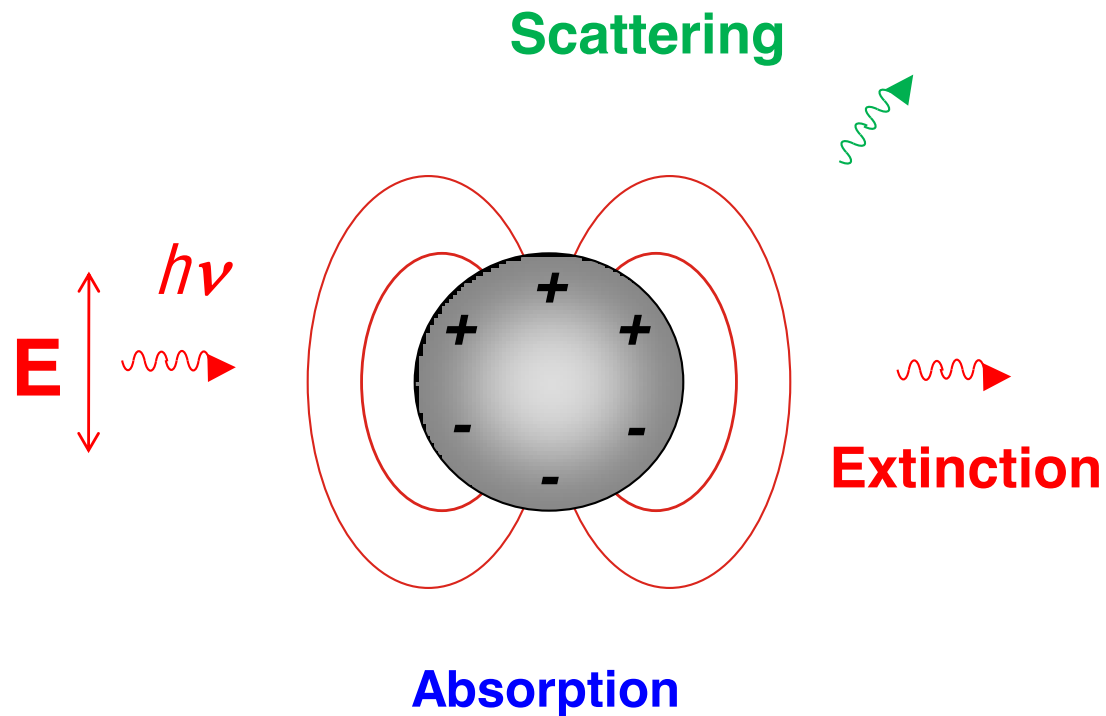
Halas, Nordlander
Plasmonic photodetector



Capasso
Antenna QCL



The simplest optical antenna: a metallic particle



Enhancement of absorption and emission:
Bringing effectively the far-field into the near-field

Metal particle plasmons

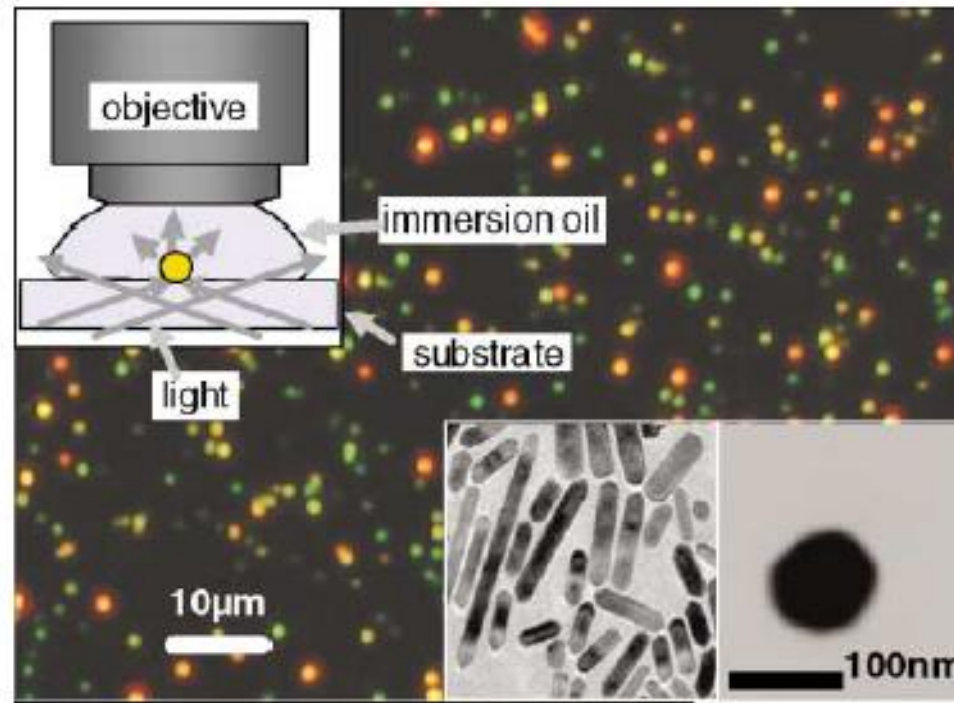
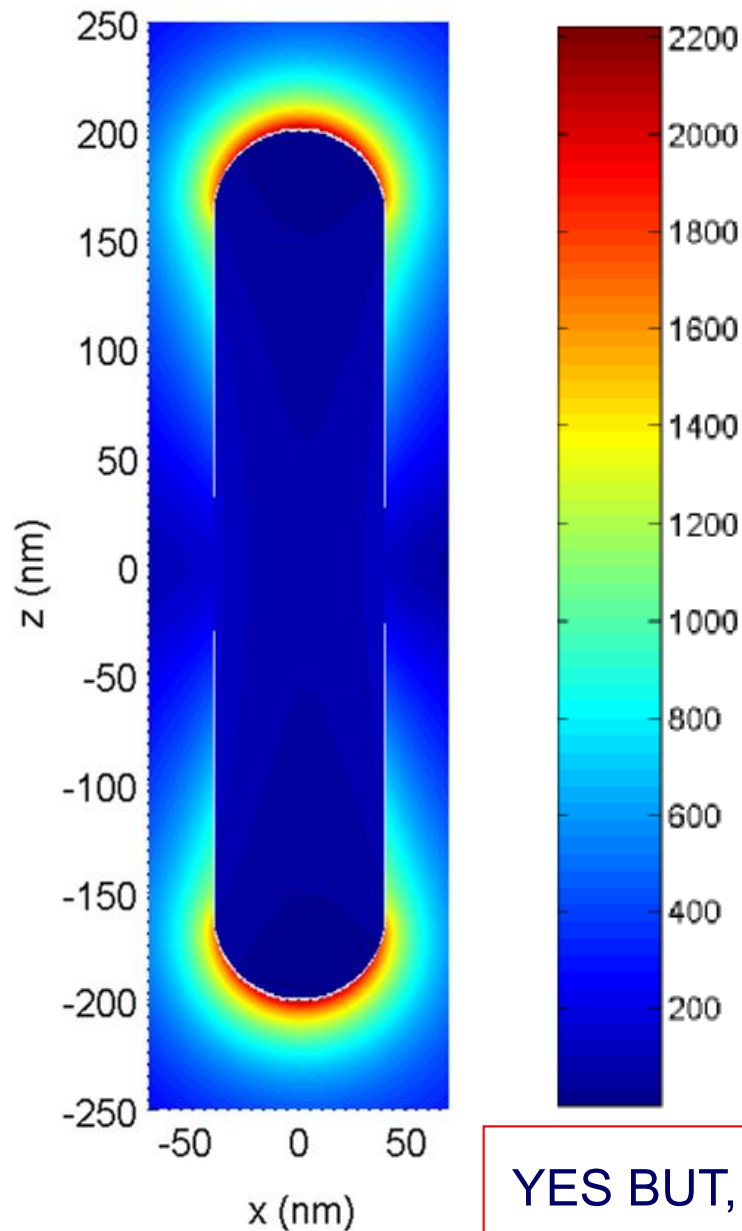


FIG. 2 (color). True color photograph of a sample of gold nanorods (red) and 60 nm nanospheres (green) in dark-field illumination (inset upper left). Bottom right: TEM images of a dense ensemble of nanorods and a single nanosphere.

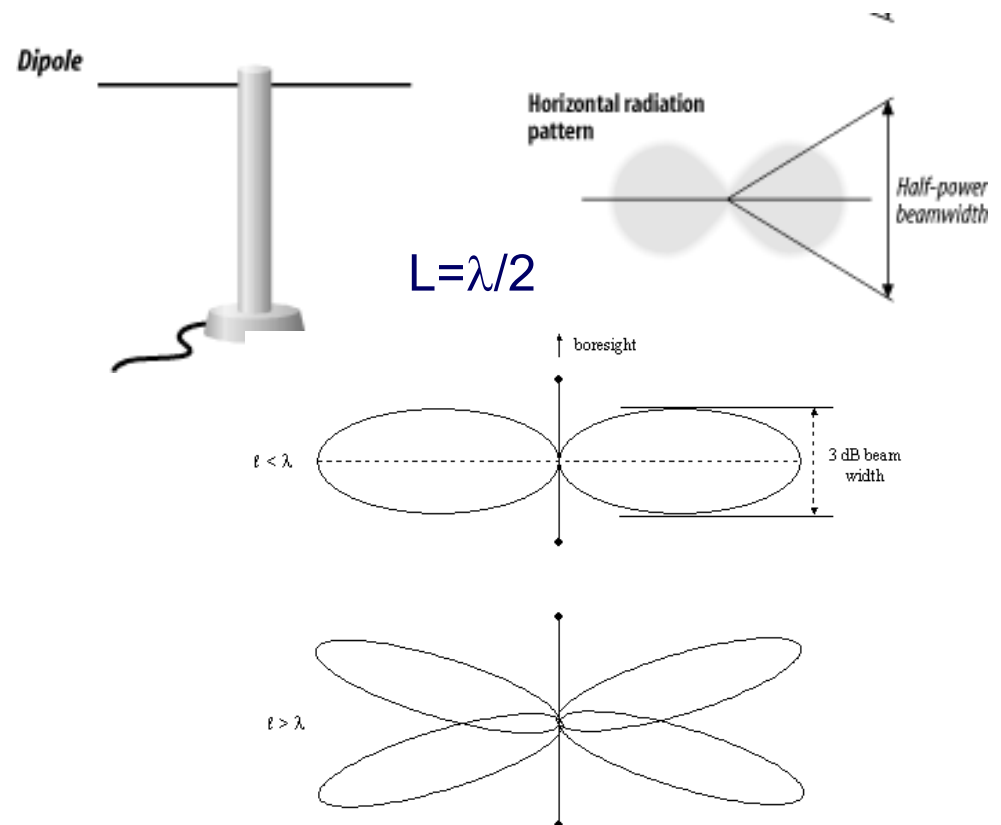
Standard textbooks:

- Kreibig, Vollmer, Optical properties of metal clusters, Springer 1995
- Bohren, Huffman, Absorption and scattering of light by small particles, Wiley 1983

Metallic nanorod as a $\lambda/2$ optical antenna



In analogy to a $\lambda/2$ radiowave antenna, we call a nanosized rod-like metallic structure a $\lambda/2$ optical antenna .



YES BUT, it is just similar, and not equal because of plasmons

Bulk plasmons

A plasmon is a collective oscillation of the conduction electrons

Bulk plasmon:

The rigid displacement of the electrons induces a dipolar moment and an electric field opposing the displacement



Newton's equation for $\delta(t)$:

Electron
density

$$nm_e \frac{d^2}{dt^2} \delta(t) = -enE(t) = -4\pi n^2 e^2 \delta(t)$$

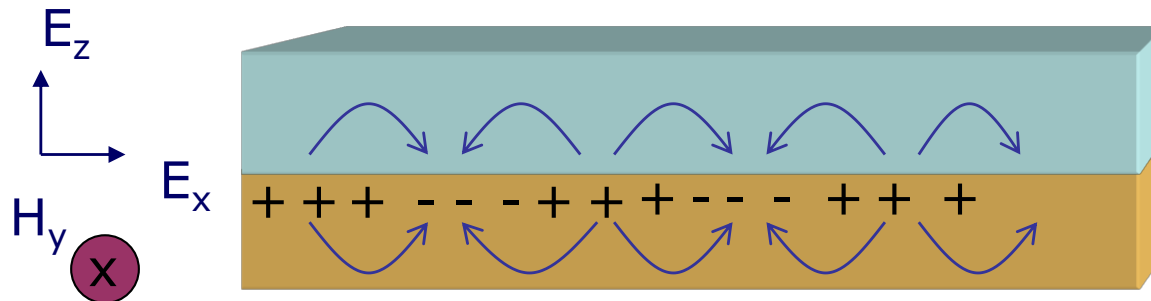
=> Harmonic oscillator

$$\omega_p = \sqrt{\frac{4\pi n_e e^2}{m_e}}$$

All the electrons are involved in the oscillation. The energy of those oscillations in typical metals might be triggered out by external probes.

Surface plasmons

Electromagnetic surface waves which exist at the interface between 2 media whose ϵ have opposite sign.

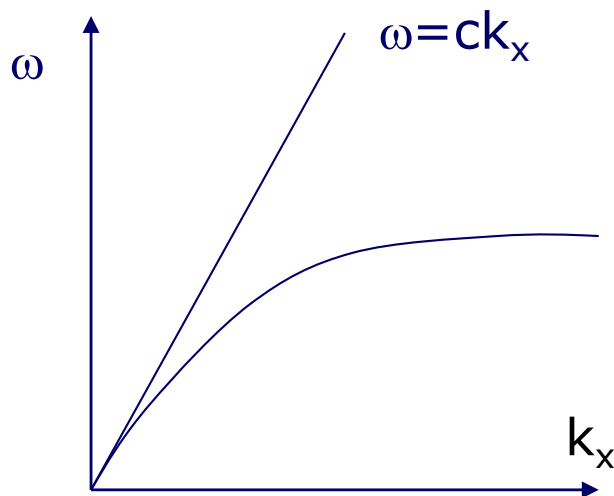


Metal ($\epsilon_1 = \epsilon_1' + i\epsilon_1''$)

Dielectric ($\epsilon_2 = \epsilon_2' + i\epsilon_2''$)

$$E^{(1)} = E_0^{(1)} e^{j(k_x x - \omega t) - \alpha^{(1)} |z|} \quad k_x = k'_x + ik''_x = \sqrt{\frac{\epsilon_1 \epsilon_2}{\epsilon_1 + \epsilon_2}} \left(\frac{\omega}{c} \right)$$

Dispersion relation



Drude model

$$\epsilon' = 1 - \frac{\omega_p^2}{\omega^2}$$

Surface plasmons

$$\omega_s = \frac{\omega_p}{\sqrt{2}}$$

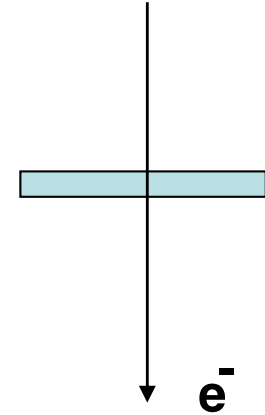
Plasma Losses by Fast Electrons in Thin Films*

R. H. RITCHIE

Health Physics Division, Oak Ridge National Laboratory, Oak Ridge, Tennessee

(Received February 7, 1957)

The angle-energy distribution of a fast electron losing energy to the conduction electrons in a thick metallic foil has been derived assuming that the conduction electrons constitute a Fermi-Dirac gas and that the fast electron undergoes only small fractional energy and momentum changes. This distribution exhibits both collective interaction characteristics and individual interaction characteristics, and is more general than the result obtained by other workers. Describing the conduction electrons by the hydrodynamical equations of Bloch, it has been shown that for very thin idealized foils energy loss may occur at a value which is less than the plasma energy while as the foil thickness decreases below $\sim v/\omega_p$ the loss at the plasma energy becomes less than that predicted by more conventional theories. The net result is an increase in the energy loss per unit thickness as the foil thickness is decreased. It is suggested that the predicted loss at subplasma energies may correspond to some of the low-lying energy losses which have been observed by experimenters using thin foils.



$$P(k_1, \omega) \rightarrow \frac{e^2 a}{\hbar \pi^2 v^2} \left\{ \frac{\text{Im}(1/\epsilon)}{(k_1^2 + \omega^2/v^2)} - \frac{2k_1}{a(k_1^2 + \omega^2/v^2)^2} \text{Im} \left(\frac{(1-\epsilon)^2}{\epsilon(1+\epsilon)} \right) \right\}$$

Now let us define

$$P(k_1, \omega) = \{ aP_\infty'(k_1, \omega) + P_b(k_1, \omega) \},$$

Now let us define

$$P(k_1, \omega) = \{ aP_\infty'(k_1, \omega) + P_b(k_1, \omega) \},$$

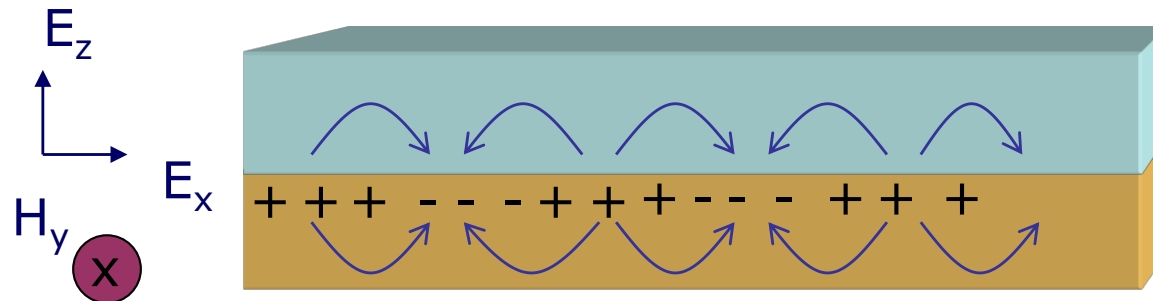
where P_∞' is the transition probability per unit foil thickness in an infinite foil and P_b is the term introduced by the boundary effect. Then one may write, inserting the expression for ϵ ,

$$P_b = \frac{e^2}{\pi^2 \hbar v^2} \frac{2k_1}{(k_1^2 + \omega^2/v^2)^2} \frac{g\omega_p^4}{\omega} \cdot \left\{ \frac{\frac{1}{4}\omega_p^2}{(\omega^2 - \frac{1}{2}\omega_p^2)^2 + g^2\omega^2} - \frac{\omega_p^2}{(\omega^2 - \omega_p^2)^2 + g^2\omega^2} \right\}. \quad (25)$$

One notes that the effect of the boundary is to cause a decrease in loss at the plasma frequency and an additional loss at $\omega = \omega_p/\sqrt{2}$. Call the probabilities for these

Surface plasmons

Electromagnetic surface waves which exist at the interface between 2 media whose ϵ have opposite sign.

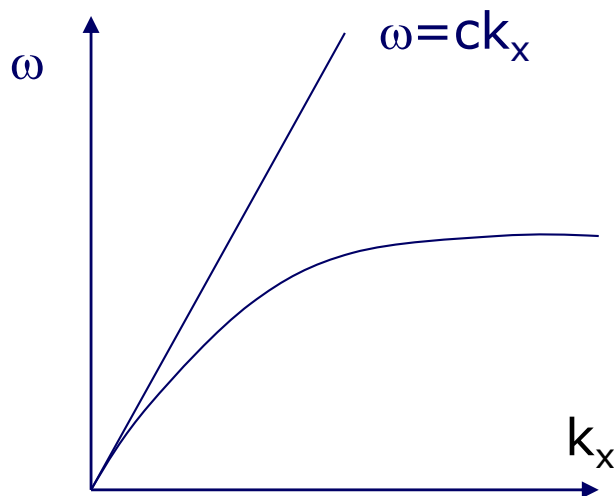


Metal ($\epsilon_1 = \epsilon_1' + i\epsilon_1''$)

Dielectric ($\epsilon_2 = \epsilon_2' + i\epsilon_2''$)

$$E^{(1)} = E_0^{(1)} e^{j(k_x x - \omega t) - \alpha^{(1)} |z|} \quad k_x = k'_x + ik''_x = \sqrt{\frac{\epsilon_1 \epsilon_2}{\epsilon_1 + \epsilon_2}} \left(\frac{\omega}{c} \right)$$

Dispersion relation



Drude model

$$\epsilon' = 1 - \frac{\omega_p^2}{\omega^2}$$

Surface plasmons

$$\omega_s = \frac{\omega_p}{\sqrt{2}}$$

Methods of SPP excitation

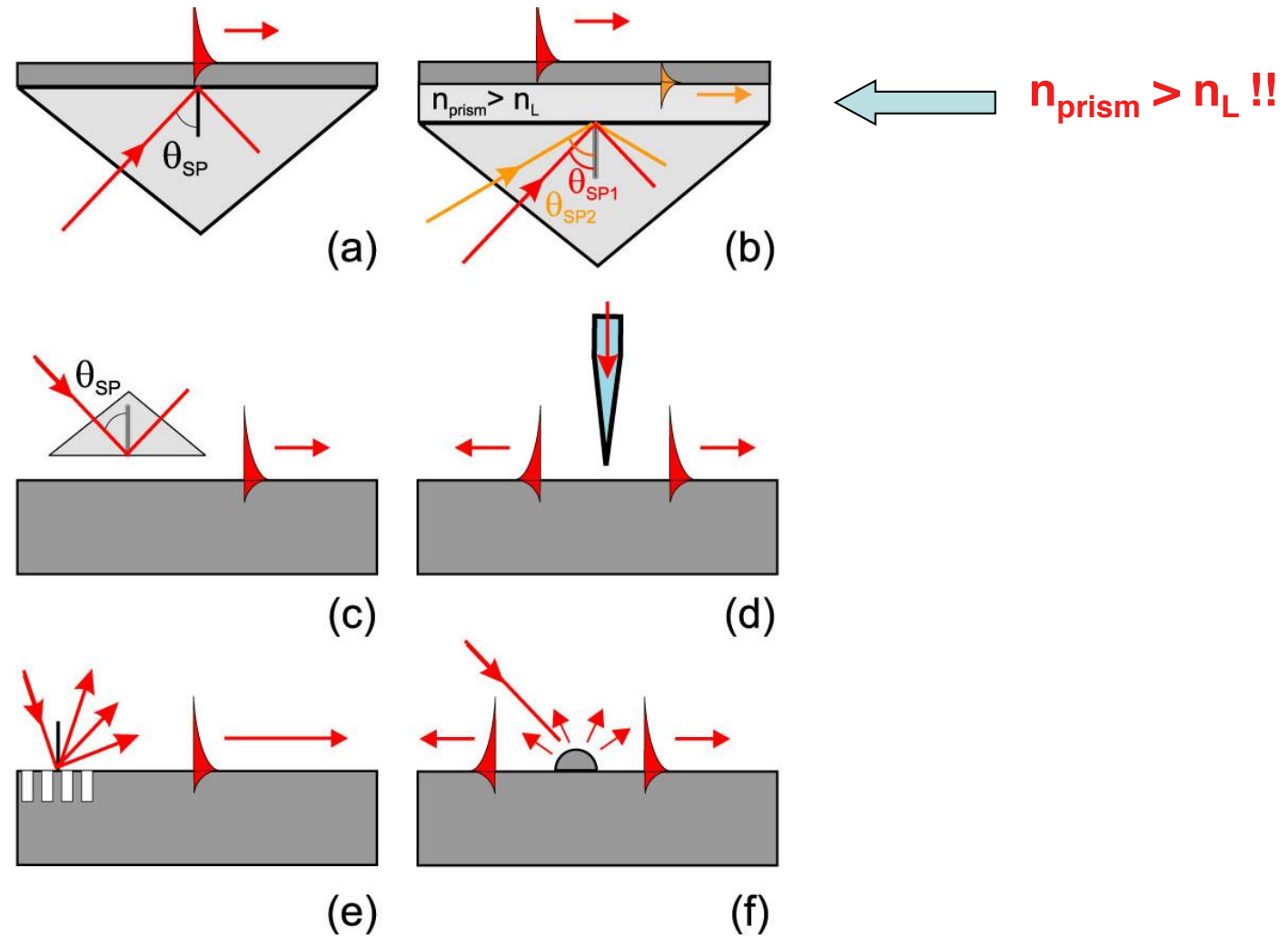


Figure 2 SPP excitation configurations: (a) Kretschmann geometry, (b) two-layer Kretschmann geometry, (c) Otto geometry, (d) excitation with an SNOM probe, (e) diffraction on a grating, and (f) diffraction on surface features.

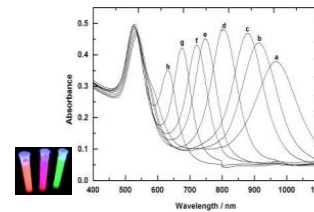
Nano-optics with localised plasmons

Characteristics

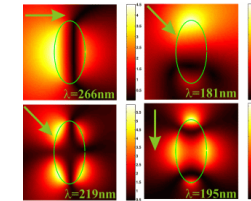
- Confined fields:
- *Nanooptics*
- Enhanced field:
- *Lighting rod effect*
- Tunability:
- *Geometry*
- Coupling:
- Wavelength range:
- *Visible → Infrared*

Resonances dependence

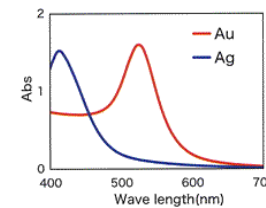
with size



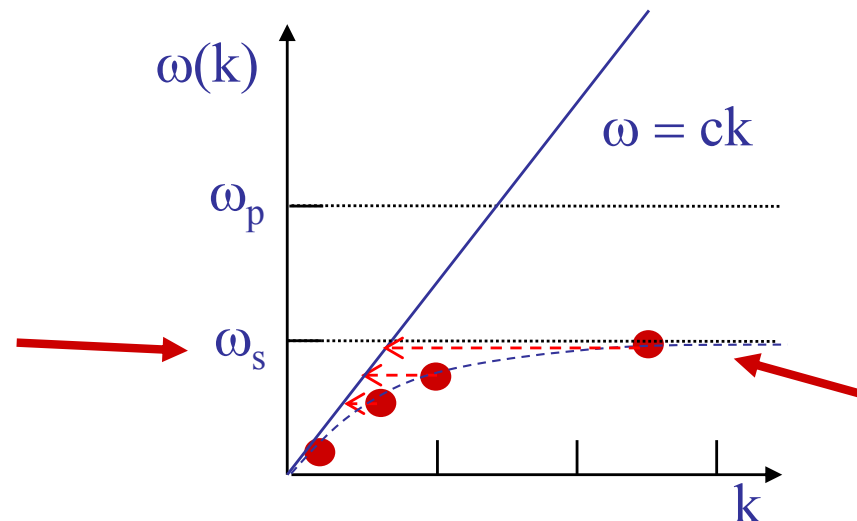
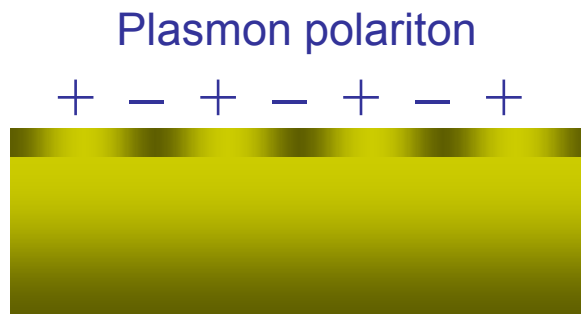
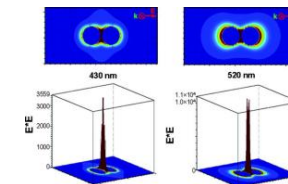
with shape



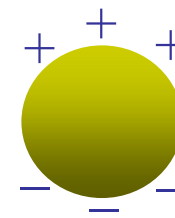
with material



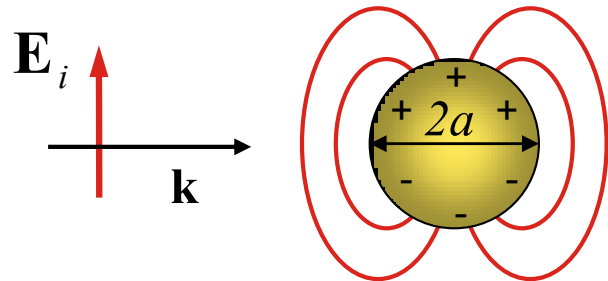
with coupling



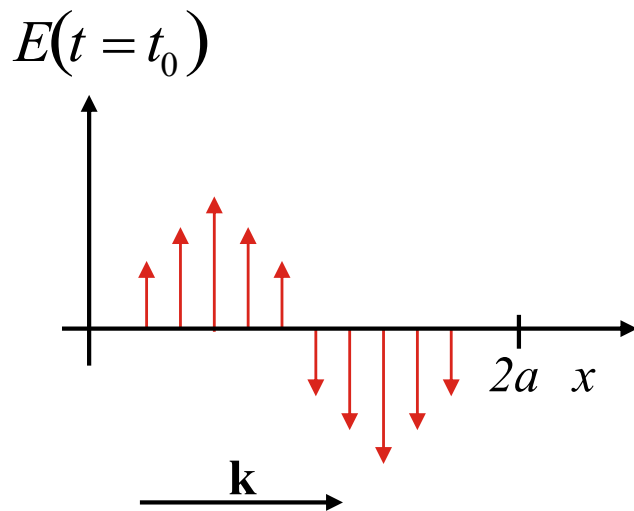
Confined plasmon



Light-particle interaction

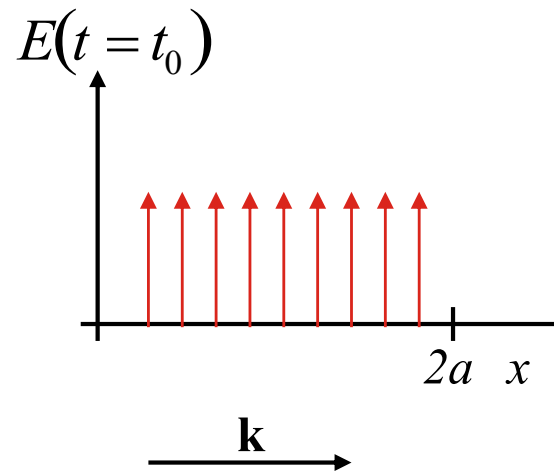


General case: $\lambda \leq a$



Phase shifts in the particles:
retardation, multipole excitations

Quasi-static case: $\lambda \gg a$



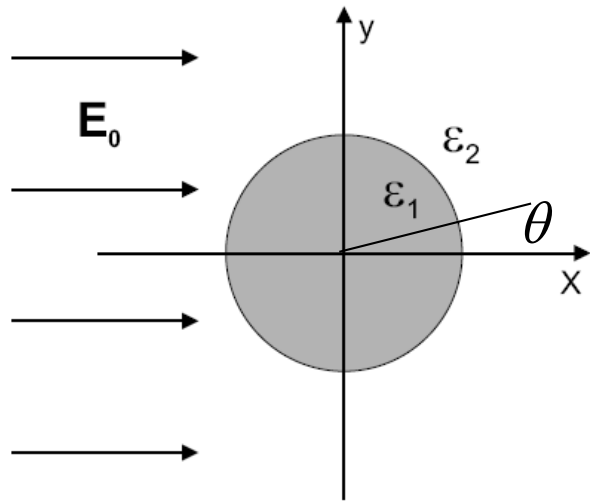
Homogeneous polarization:
All points of an object respond simultaneously
to the incoming (exciting) field.

⇒ Helmholtz eq. reduces to Laplace
equation:

$$\nabla^2 \Phi = 0$$

⇒ el. field: $\mathbf{E} = -\nabla \Phi$

Small sphere



The electric fields inside (E_1) and outside (E_2) the sphere can be obtained from the scalar potentials $\Phi = \Phi(r, \theta, \varphi)$

$$E_1 = -\nabla\Phi_1 \quad \text{with} \quad \nabla^2\Phi_1 = 0$$

$$E_2 = -\nabla\Phi_2 \quad \text{with} \quad \nabla^2\Phi_2 = 0$$

$$\Phi_2 = \Phi_{scatter} + \Phi_0$$

Solve Laplace equation in spherical coordinates:

$$\frac{1}{r^2 \sin \theta} \left[\sin \theta \frac{\partial}{\partial r} \left(r^2 \frac{\partial}{\partial r} \right) + \frac{\partial}{\partial \theta} \left(\sin \theta \frac{\partial}{\partial \theta} \right) + \frac{1}{\sin \theta} \frac{\partial^2}{\partial \varphi^2} \right] \Phi(r, \theta, \varphi) = 0$$

Boundary conditions:

$$\frac{\partial\Phi_1}{\partial\theta} = \frac{\partial\Phi_2}{\partial\theta} \quad (r = a)$$

continuity of the tangential electric fields

$$\varepsilon_1 \frac{\partial\Phi_1}{\partial r} = \varepsilon_2 \frac{\partial\Phi_2}{\partial r} \quad (r = a)$$

continuity of the normal component of the electric displacement

Small sphere

Homogeneous electric field along x-direction: $\Phi_0 = -E_0 x = -E_0 r \cos \theta$

The following potentials satisfy the Laplace equation and boundary conditions:

$$\Phi_1 = -E_0 \frac{3\varepsilon_2}{\varepsilon_1 + 2\varepsilon_2} r \cos \theta$$

$$\Phi_2 = -E_0 r \cos \theta + E_0 \frac{\varepsilon_1 - \varepsilon_2}{\varepsilon_1 + 2\varepsilon_2} a^3 \frac{\cos \theta}{r^2}$$

From $\mathbf{E} = -\nabla\Phi$ we obtain

$$\mathbf{E}_1 = E_0 \frac{3\varepsilon_2}{\varepsilon_1 + 2\varepsilon_2} (\cos \theta \mathbf{e}_r - \sin \theta \mathbf{e}_\theta) = E_0 \frac{3\varepsilon_2}{\varepsilon_1 + 2\varepsilon_2} \mathbf{e}_x$$

$$\mathbf{E}_2 = E_0 (\cos \theta \mathbf{e}_r - \sin \theta \mathbf{e}_\theta) + \frac{\varepsilon_1 - \varepsilon_2}{\varepsilon_1 + 2\varepsilon_2} \frac{a^3}{r^3} E_0 (2 \cos \theta \mathbf{e}_r + \sin \theta \mathbf{e}_\theta)$$

The field is independent of the azimuth angle φ which is a result of the symmetry implied by the direction of the applied electric field.

Small sphere

Small sphere: $\Phi_2 = -E_0 r \cos \theta + E_0 \frac{\epsilon_1 - \epsilon_2}{\epsilon_1 + 2\epsilon_2} a^3 \frac{\cos \theta}{r^2}$

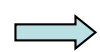
Dipole: $\Phi_{dipole} = \frac{\rho \cos \theta}{4\pi\epsilon_2 r^2}$

→ The field outside the sphere is the superposition of the applied field and the field of an ideal dipole at the sphere origin

The dipole moment is given by

$$\rho = 4\pi\epsilon_0\epsilon_2 a^3 \frac{\epsilon_1 - \epsilon_2}{\epsilon_1 + 2\epsilon_2} E_0$$

Generally the dipole moment is defined by $\rho = \epsilon_0\epsilon_2\alpha E_0$



Polarizability of the sphere:

$$\alpha = 4\pi a^3 \frac{\epsilon_1 - \epsilon_2}{\epsilon_1 + 2\epsilon_2}$$

Small sphere

We can describe the light scattering of a small sphere by plane wave scattering at an ideal point dipole with dipole moment derived on the previous slides. The dipole field is given by:

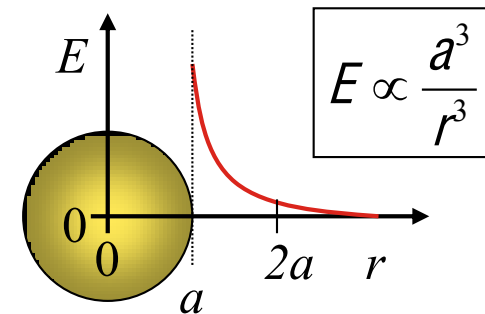
$$E(\mathbf{r}) = \frac{1}{4\pi\epsilon_0} \frac{e^{ikr}}{r} \left\{ k^2 [(\mathbf{n} \times \mathbf{p}) \times \mathbf{n}] + \frac{1}{r} \left(\frac{1}{r} - ik \right) [3\mathbf{n}(\mathbf{n} \cdot \mathbf{p}) - \mathbf{p}] \right\} e^{i\omega t} \quad \text{with} \quad \mathbf{n} = \frac{\mathbf{r}}{r}$$

Near-field zone:
 $kr \ll 1$ ($r \ll \lambda$)

$$E(\mathbf{r}) = \frac{1}{4\pi\epsilon_0} \frac{3\mathbf{n}(\mathbf{n} \cdot \mathbf{p}) - \mathbf{p}}{r^3} e^{-i\omega t}$$

electrostatic dipole field

harmonic time dependency

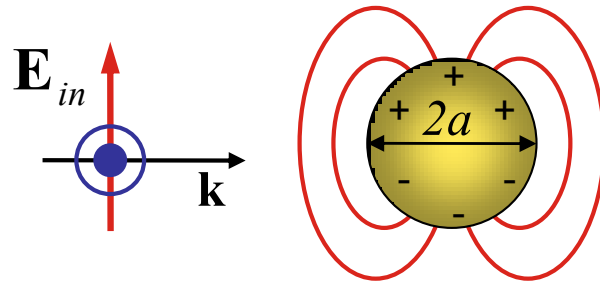


Radiation zone:
 $kr \gg 1$ ($r \gg \lambda$)

$$E(\mathbf{r}) = \frac{(\mathbf{n} \times \mathbf{p}) \times \mathbf{n}}{r} \frac{k^2}{4\pi\epsilon_0} e^{i(kr - \omega t)}$$

propagating wave

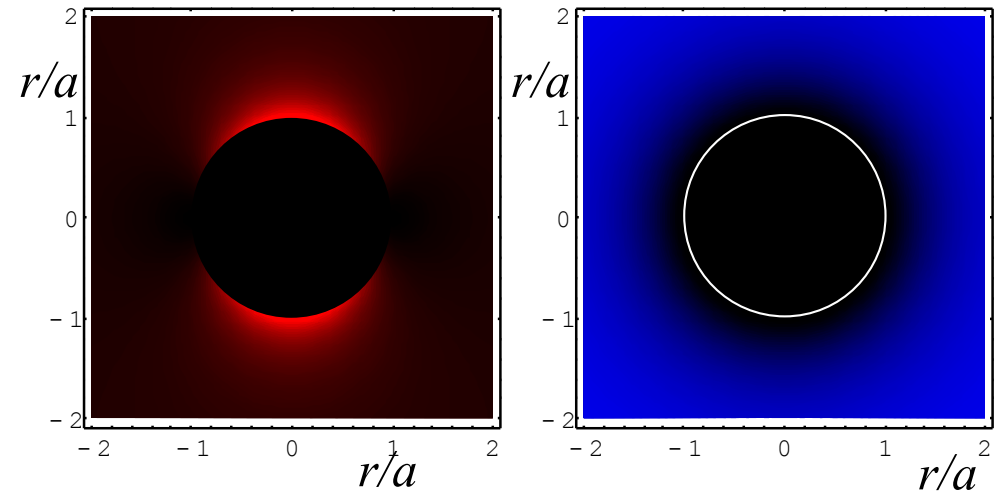
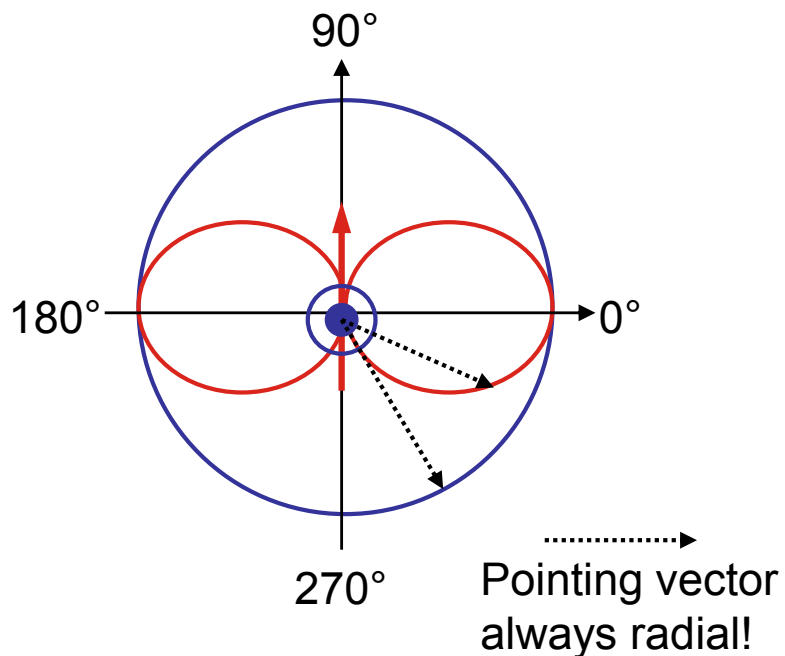
Far- and near-field calculations for a sphere $a \ll \lambda$



Near-field scattering

$$I = |\mathbf{E}_{in} + \mathbf{E}_{particle}|^2$$

Far-field scattering (transverse fields)



Pointing vector is
not always radial

Optical cross sections of small spheres

Integrating the Poynting vector \mathbf{S}_{sca} (\mathbf{S}_{abs}) over a close spherical surface we obtain the totally scattered (absorbed) power P_{sca} (P_{abs}) from which we can calculate the scattering (absorption) cross section $C_{\text{sca}} = P_{\text{sca}}/I_i$ ($C_{\text{abs}} = P_{\text{abs}}/I_i$):

Scattering cross section:

$$C_{\text{sca}} = \frac{8\pi}{3} k^4 a^6 \left| \frac{\varepsilon - \varepsilon_m}{\varepsilon + 2\varepsilon_m} \right|^2 = \frac{k^4}{6\pi} |\alpha|^2$$

$$\Rightarrow C_{\text{sca}} \propto \frac{a^6}{\lambda^4}$$

Absorption cross section:

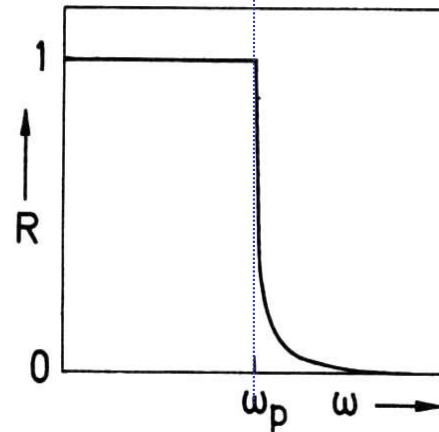
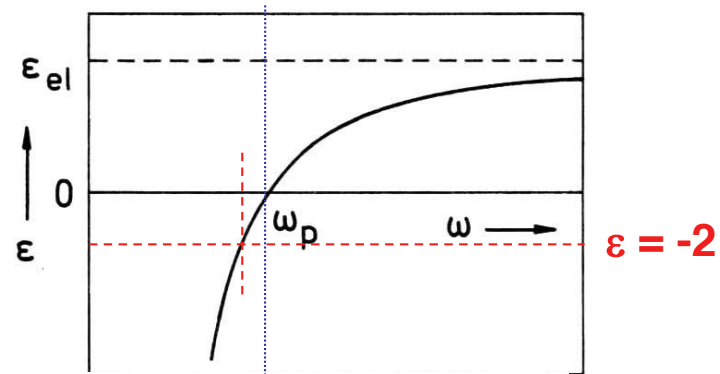
$$C_{\text{abs}} = 4\pi k a^3 \text{Im} \left\{ \frac{\varepsilon - \varepsilon_m}{\varepsilon + 2\varepsilon_m} \right\} = k \text{Im}\{\alpha\}$$

$$\Rightarrow C_{\text{abs}} \propto \frac{a^3}{\lambda}$$

- stronger scattering at shorter wavelength (Rayleigh scattering, blue sky)
- for large particle extinction is dominated by scattering whereas for small particles it is associated with absorption
- scattering of single particles <10nm is difficult to measure (low signal/noise and low signal/background)

Dielectric function of metals

Collective free electron oscillations (plasmons)

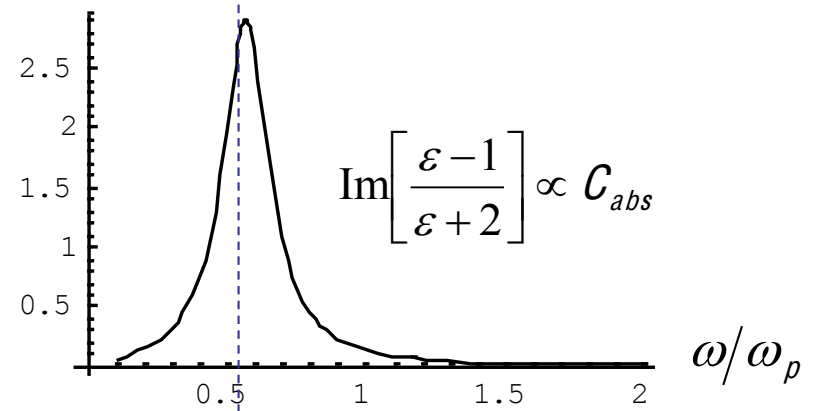
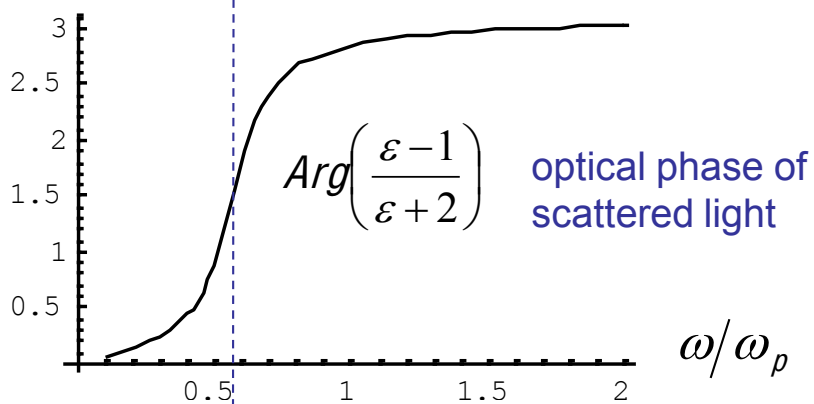
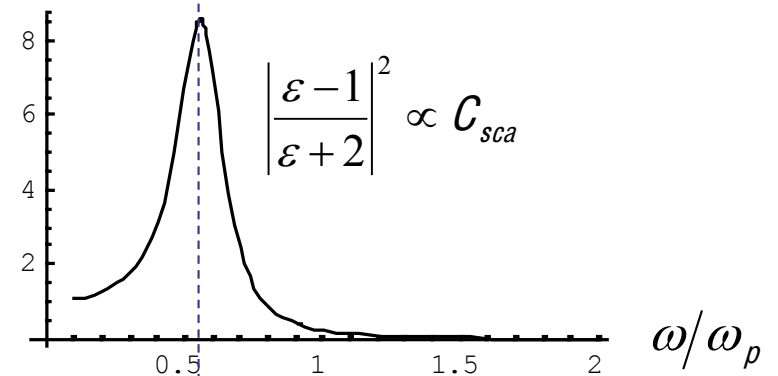
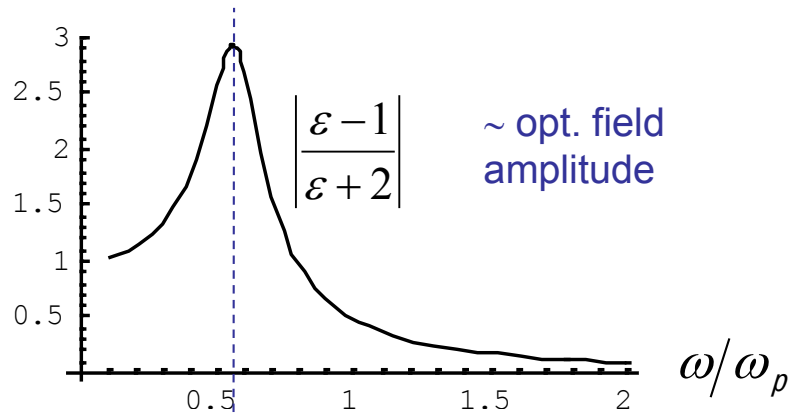
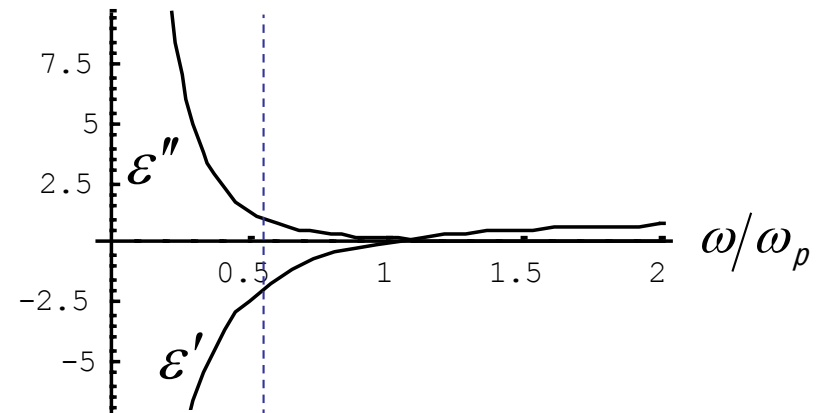


↑
plasma frequency
(longitudinal oscillation)

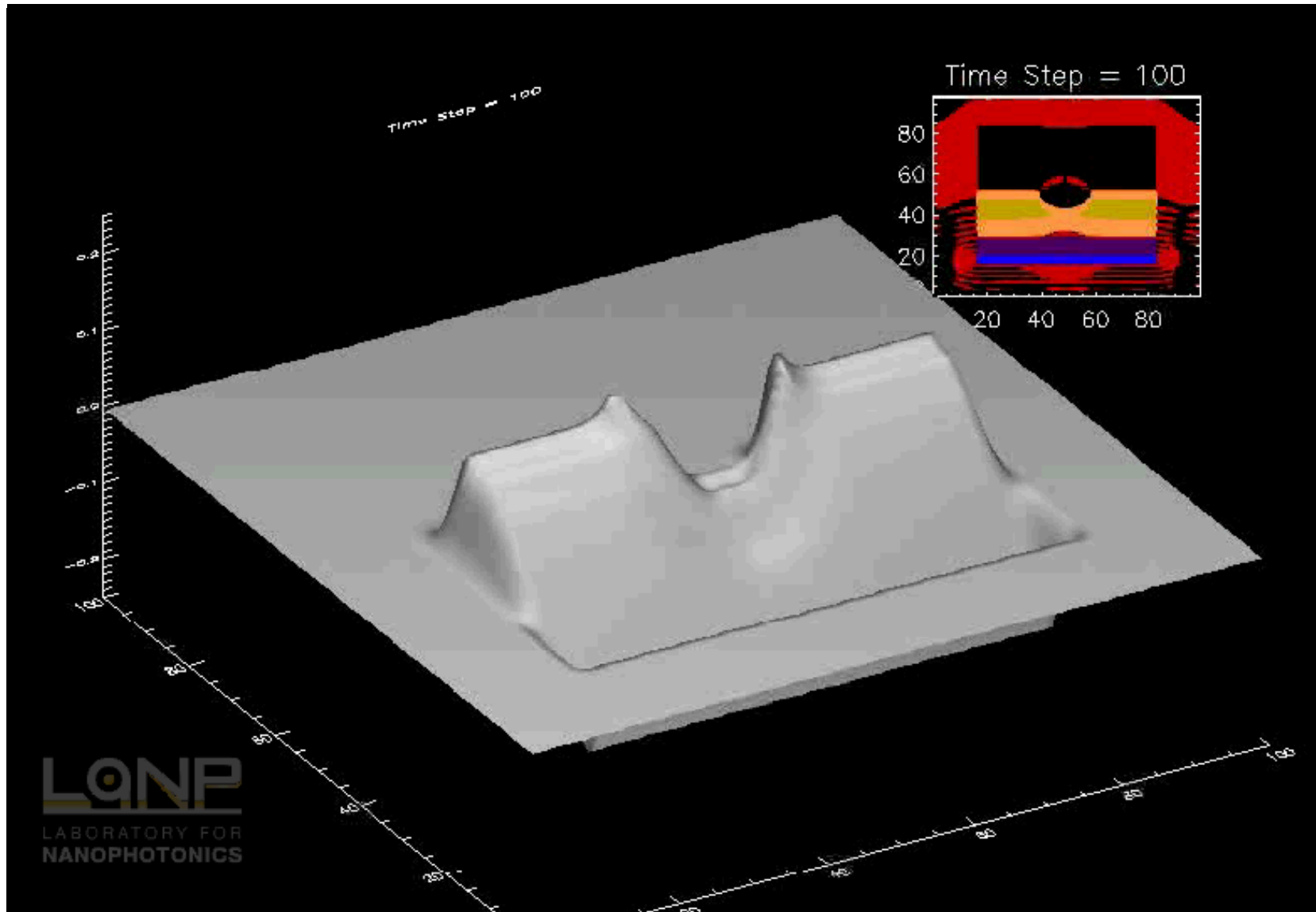
Optical cross sections of small spheres

Drude model

$$\epsilon = 1 - \frac{\omega_p^2}{\omega^2 + 0.2i\omega}$$



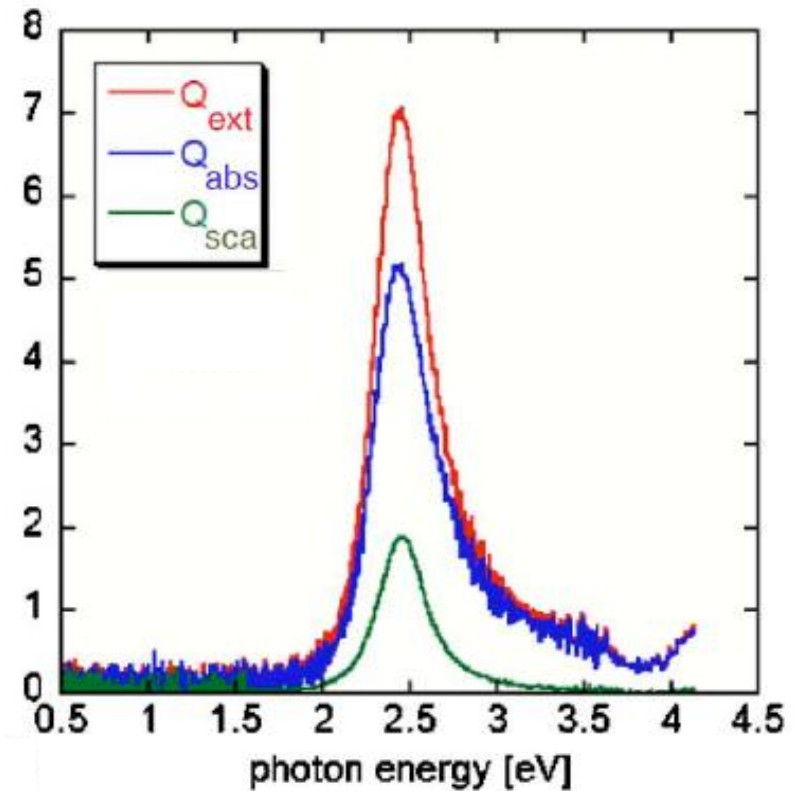
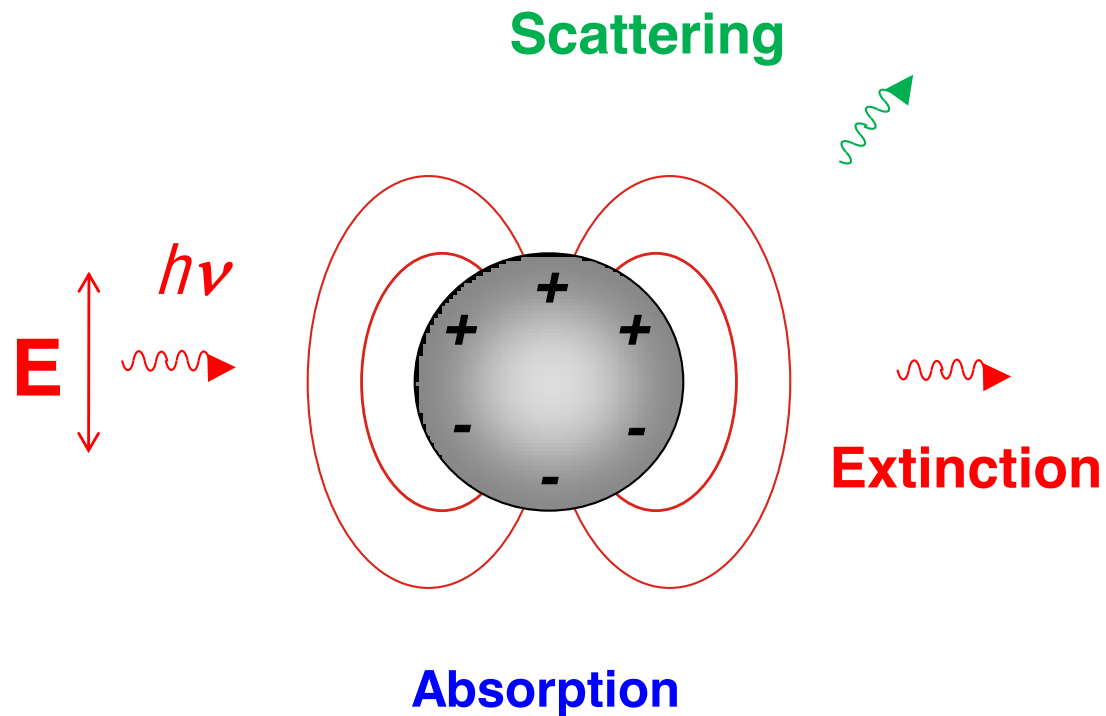
Excitation of a plasmon by a pulse



Localised Surface Plasmon: a swimming pool of e^-

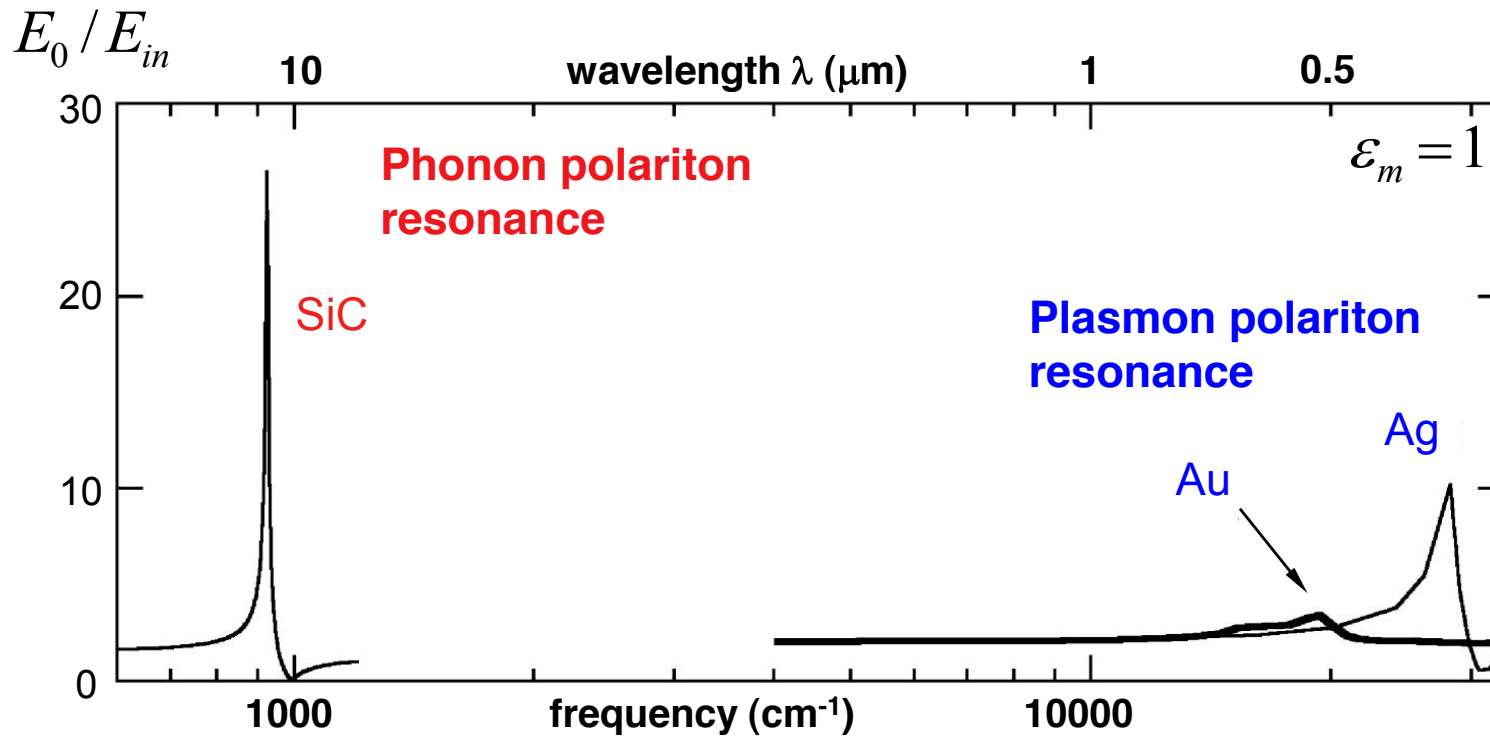
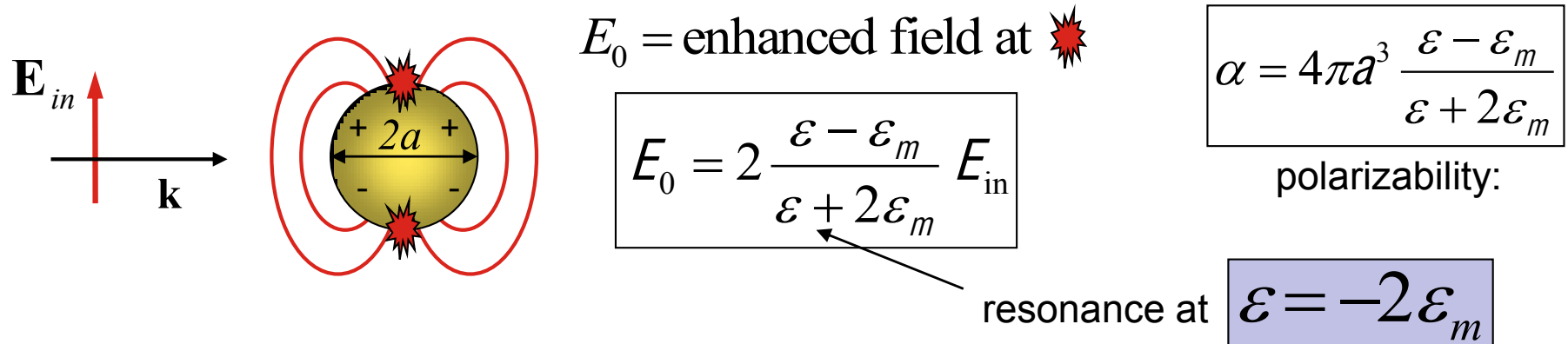


The simplest optical antenna: a metallic particle



Enhancement of absorption and emission:
Bringing effectively the far-field into the near-field

Small particle resonances



Nanotechnology with plasmonics: before the nanorevolution

Lycurgus Cup

(British Museum; 4th century AD)



Illumination: from outside



from inside

(strong absorption at and below 520 nm)

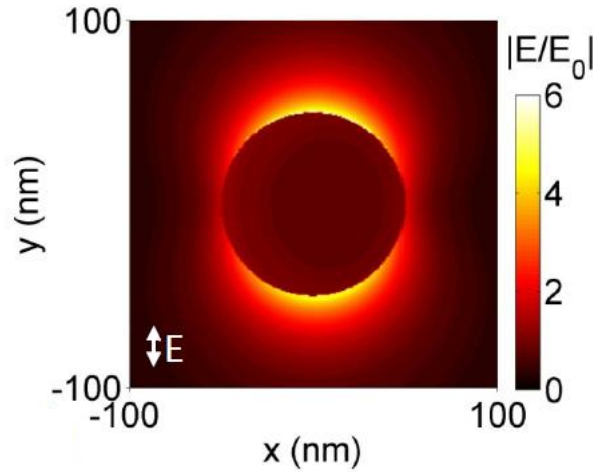
Extinction vs. scattering



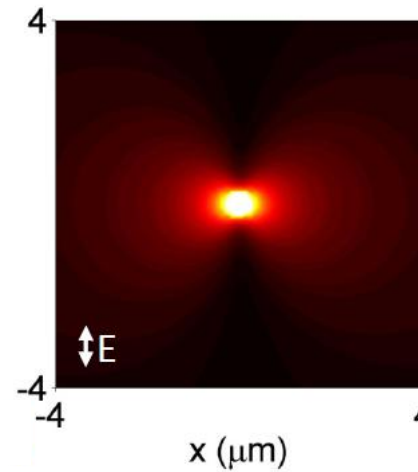
Ancient roman Lycurgus cup illuminated by a light source from behind. Light absorption by the embedded gold particles leads to a red color of the transmitted light whereas scattering at the particles yields a greenish color. From <http://www.thebritishmuseum.ac.uk/science/lycurguscup/sr-lycugus-p1.html>.

Near-field versus far-field

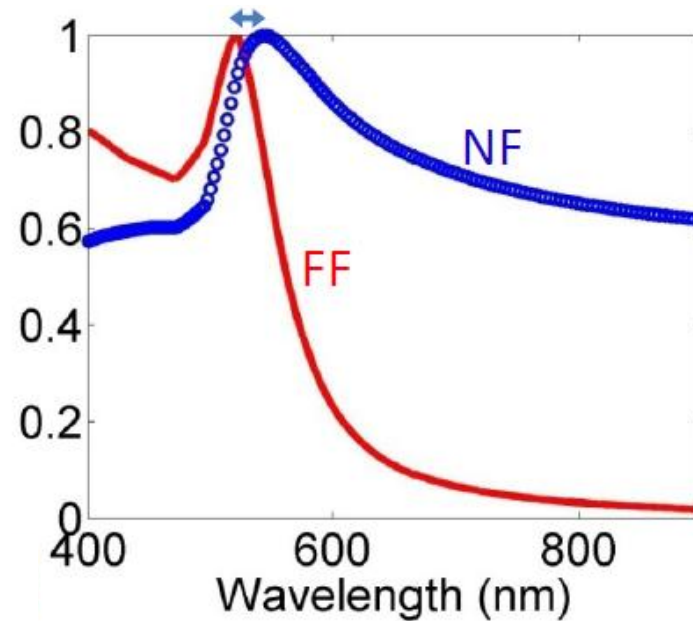
Near-field distribution



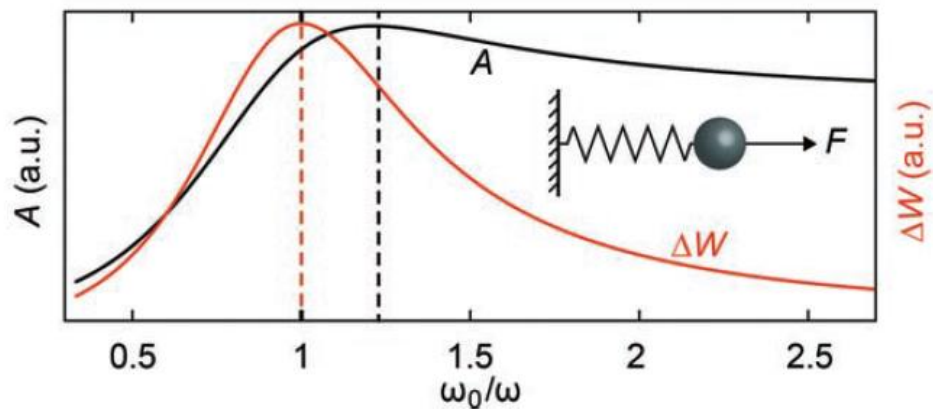
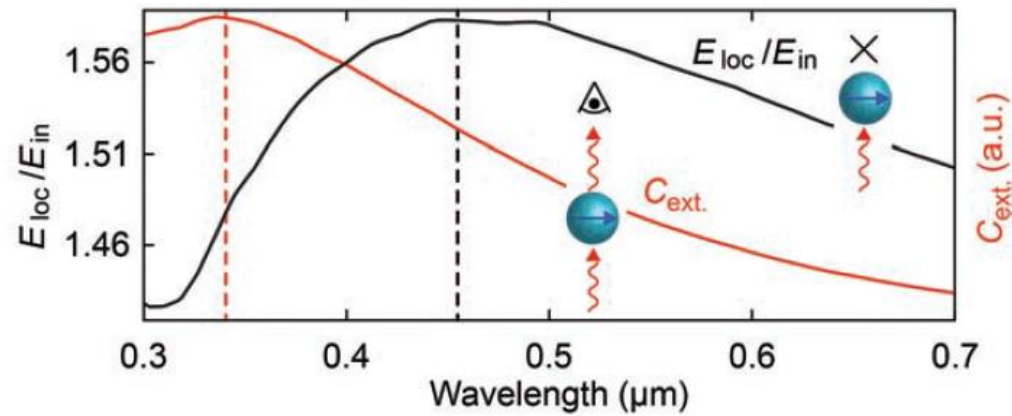
Far-field distribution



Spectral information



Near-field versus far-field



$$\ddot{x} + \gamma \dot{x} + \omega_0^2 x = F/m \cos \Omega t$$

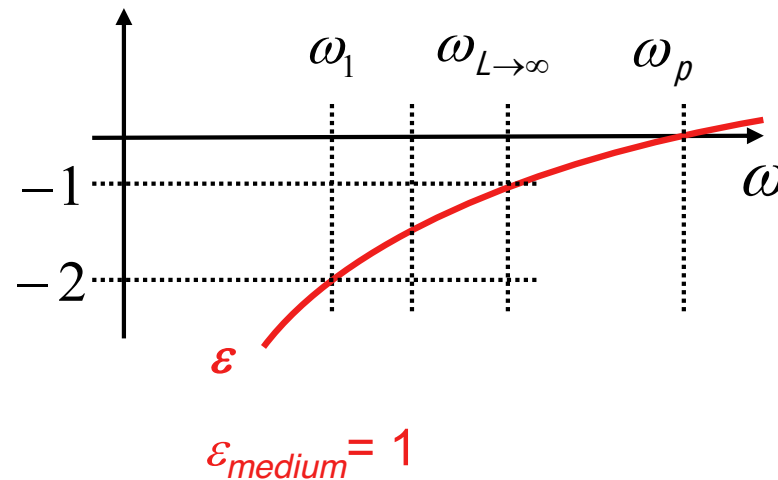
$$A = [(\omega_0^2 - \Omega^2)^2 + \gamma^2 \Omega^2]^{-1/2}$$

$$\Delta W = F^2 \Omega^2 \gamma / (2m [(\omega_0^2 - \Omega^2)^2 + \gamma^2 \Omega^2])$$

Higher multipole resonances in quasistatic limit

In the quasistatic limit the Mie theory yields the resonance positions of the higher multipoles at

$$\varepsilon_L = -\varepsilon_{\text{medium}} \frac{l+1}{l} \quad \xrightarrow{\text{Drude}} \quad \omega_L = \omega_p \frac{1}{\sqrt{1 + \frac{l+1}{l} \varepsilon_{\text{medium}}}}$$

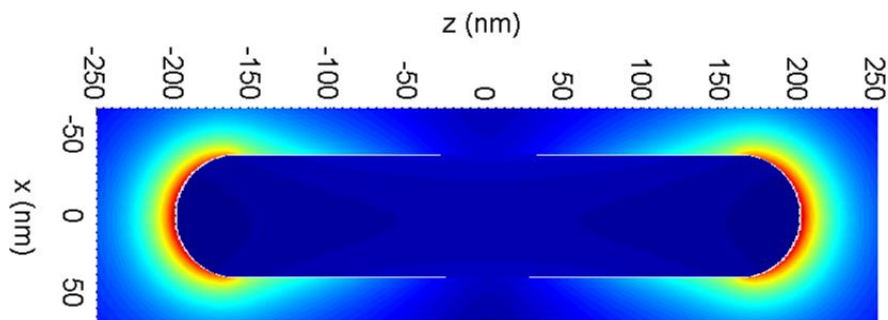
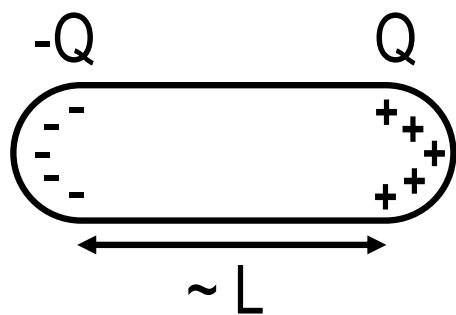


However, higher multipoles in the quasistatic limit are negligible compared to the dipole contribution ($l=1$)

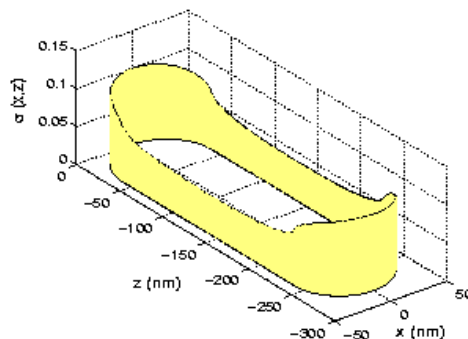
Higher order modes: $l=1, 2, 3, 4, \dots$

Antenna modes:
 $D=80\text{nm}, L=200\text{nm}; \text{ ratio}=2.5$

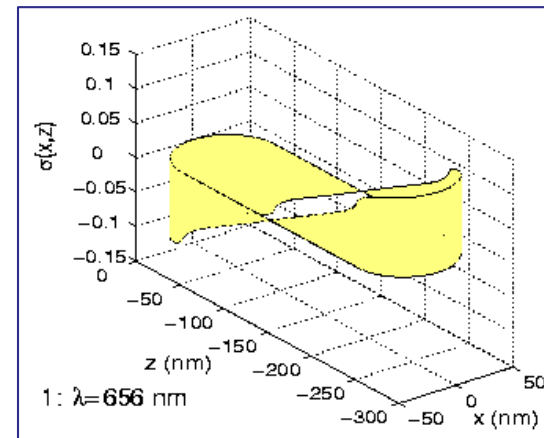
Dipole response:
 $L \propto \lambda/2$



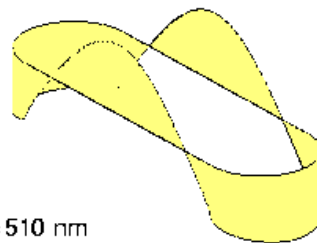
Aizpurua et al. Physical Review B 71, 235420 (2005)



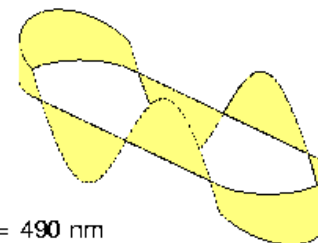
0: $\lambda=8814$ nm



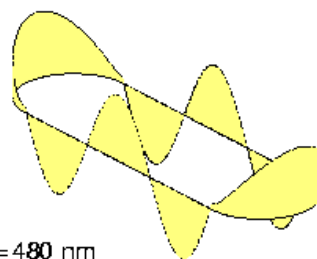
1: $\lambda=656$ nm



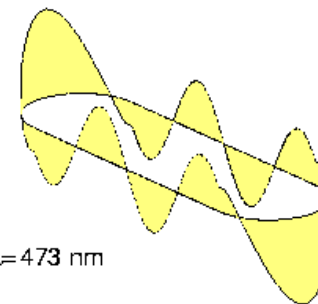
2: $\lambda=510$ nm



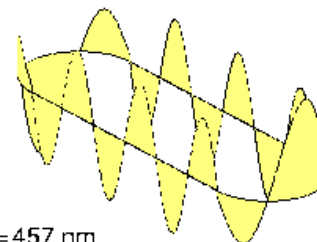
3: $\lambda=490$ nm



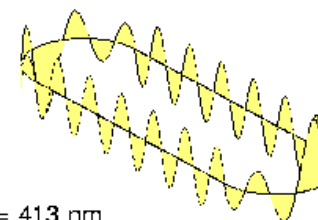
4: $\lambda=480$ nm



5: $\lambda=473$ nm



9: $\lambda=457$ nm

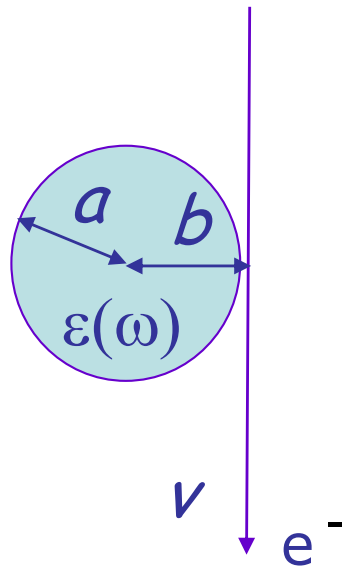


19: $\lambda=413$ nm

An alternative to excite high order modes in a sphere

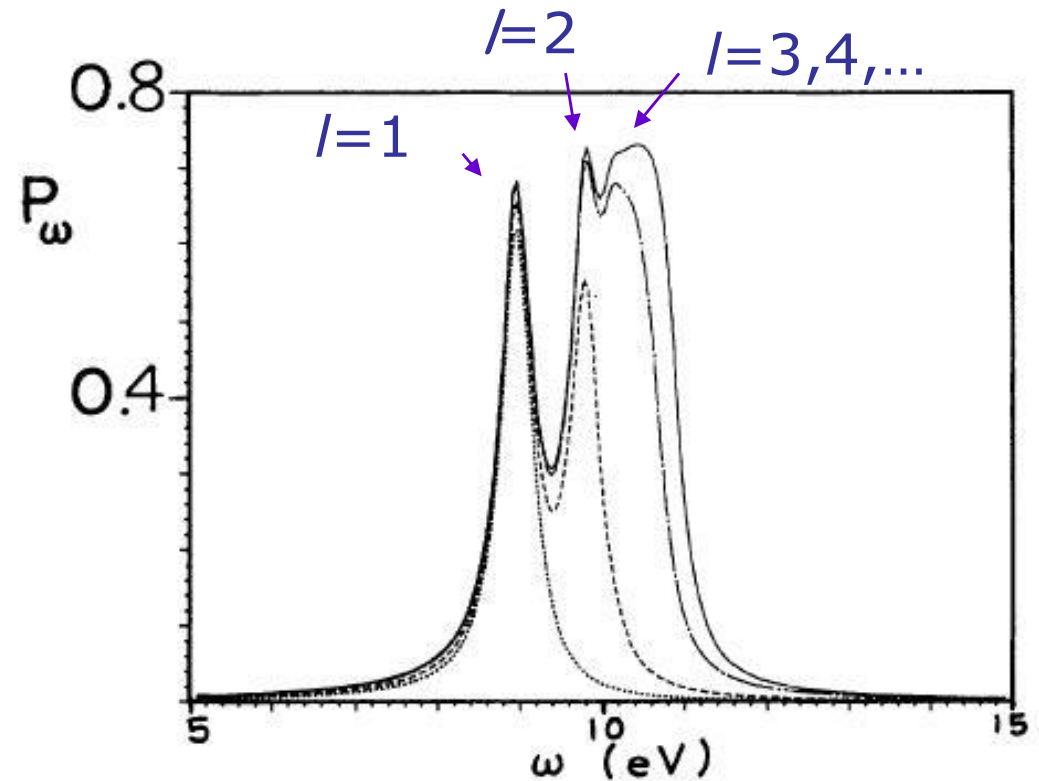
EELS in nanoparticles

Ferrell and Echenique, PRL 55, 1526 (1985)



$$\alpha_l(\omega) = \frac{\epsilon(\omega) - 1}{\epsilon(\omega) + (l+1)/l} a^3$$

$$P_\omega(a, b, v) = \frac{4q^2}{\pi v^2 a^2} \sum_{l=0}^{\infty} \sum_{m=0}^l A_{lm} \left(\frac{\omega a}{v} \right)^{2l} K_m^2 \left(\frac{\omega b}{v} \right) \text{Im}[\alpha_l(\omega)]$$



Probability of losing energy $h\omega$ for a 50-keV electron moving at grazing incidence on an aluminum sphere of radius $a=10\text{nm}$

Mie-theory

2.1.3 Exact Electrodynamical Calculation of Spherical Metal Clusters (Mie Theory) Kreibig/Vollmer

The above discussion of the *quasi-static regime* serves as a first rough estimate which only holds for sufficiently small particles and needs to be extended considerably in order to account for larger particle sizes and particle-size distributions.

The general solution of the diffraction problem of a single sphere of arbitrary material within the frame of electrodynamics was first given by Mie in 1908 [2.19]. He applied Maxwell's equations with appropriate boundary conditions in spherical coordinates ~~using multipole expansions of the incoming electric and magnetic fields. Input parameters were the particle size and the~~ optical functions of the particle material and of the surrounding medium. His solution was based upon the determination of scalar electromagnetic potentials from which the various fields were derived. In particular there are two sets of potentials Π , solving the wave equation

$$\Delta \Pi + |\mathbf{k}|^2 \Pi = 0 \quad (2.15a)$$

in spherical coordinates: $\Pi_{e,m}^{\text{inc}}$ of the incident plane wave
 $\Pi_{e,m}^{\text{in}}$ of the wave inside the cluster
 $\Pi_{e,m}^{\text{sca}}$ of the outgoing scattered wave

The indices e and m indicate the sets of *electrical* and *magnetical* partial waves, respectively. The solutions can be separated in spherical coordinates

$$\Pi = R(r)\Theta(\theta)\Phi(\phi) \quad (2.15b)$$

and have the form

$$\Pi = \{\text{cylindrical fct.}\} \cdot \{\text{Legendre spherical fct.}\} \cdot \{\text{trigonometric fct.}\} \quad (2.15c)$$

The relevant parameter in all formulas is the size parameter $x = |\mathbf{k}|R$ which distinguishes the regime of geometrical optics ($x \gg 1$) from the one important for clusters ($x \ll 1$) (a compressed description is given in [2.9]).

Mie-theory is an electrodynamic theory for optical properties of spherical particles. The solution is divided into two parts: the electromagnetic one which is treated from first principles (Maxwell equations) and the material problem which is solved by using phenomenological dielectric functions taken from experiments or model calculations

See also Bohren/Huffman

Mie theory - results

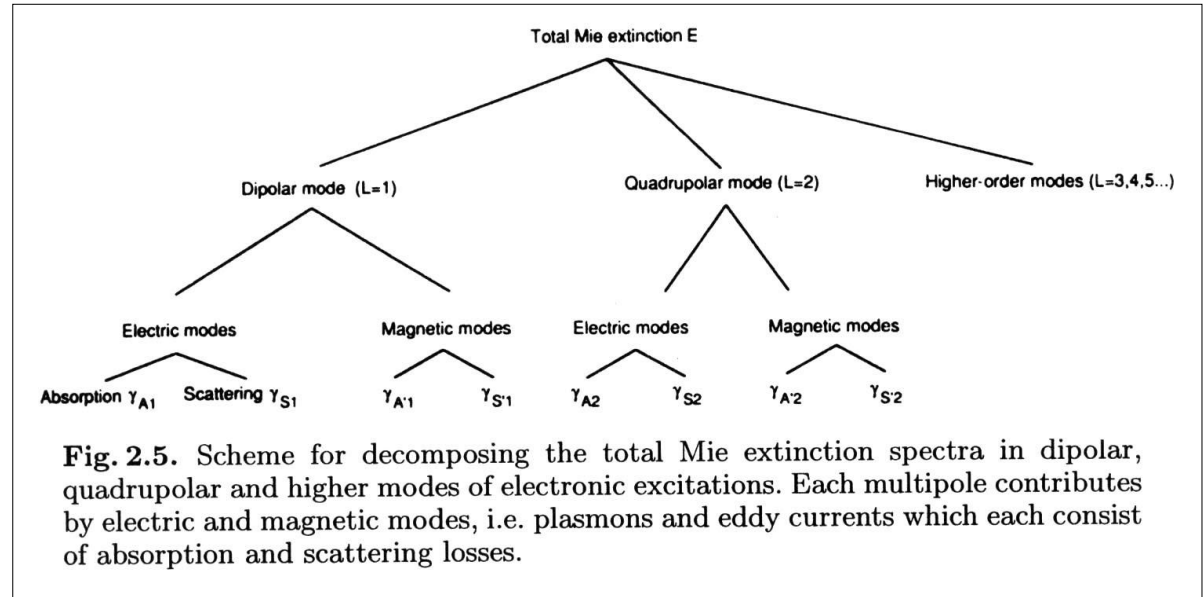
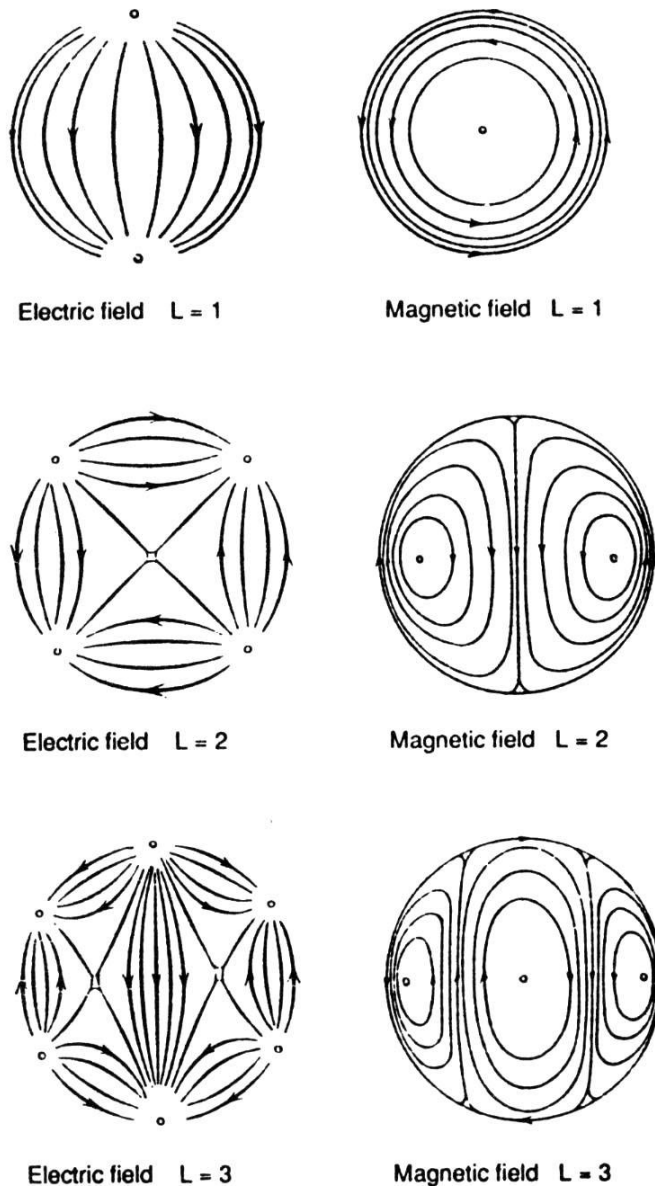


Fig. 2.5. Scheme for decomposing the total Mie extinction spectra in dipolar, quadrupolar and higher modes of electronic excitations. Each multipole contributes by electric and magnetic modes, i.e. plasmons and eddy currents which each consist of absorption and scattering losses.

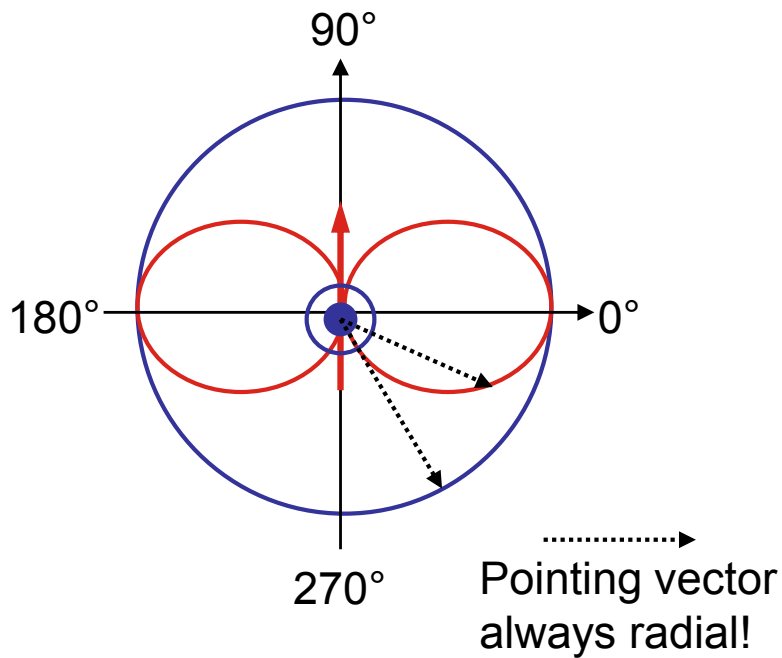
Fig. 2.6. Electric and magnetic fields far away from the clusters, of the $L = 1, 2,$ and 3 electric partial wave, i.e. the electric dipole, quadrupole, and octupole mode. The same field distributions hold for the magnetic partial waves, if electric and magnetic fields are interchanged (after [2.19]).

Fig. 2.6 shows farfield distribution at the surface of a large sphere centered at the small cluster

Kreibig/Vollmer

Scattering characteristics (far-field)

Small particle



Large particle (Mie calculation)

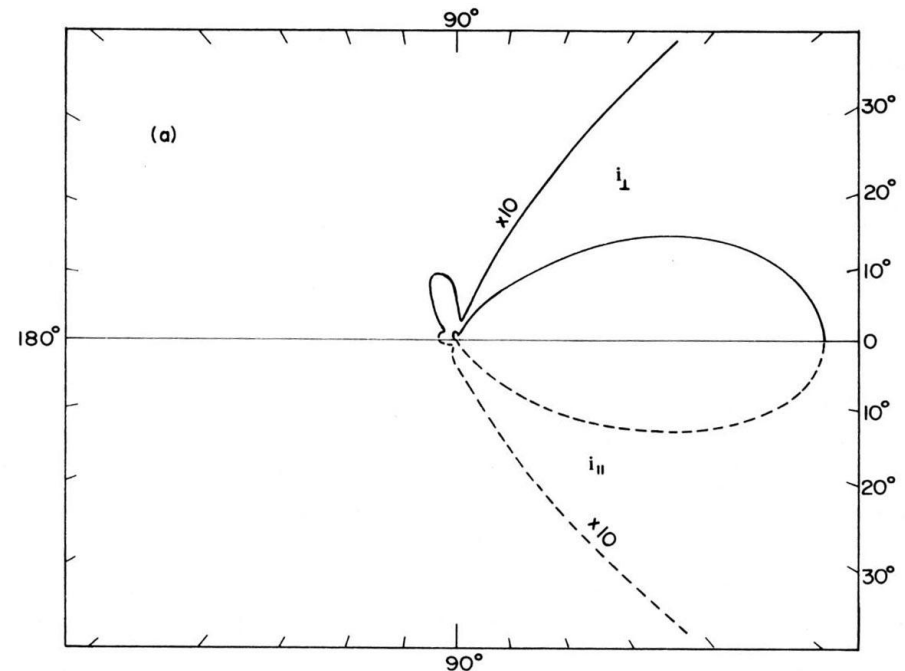
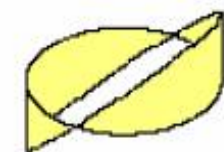
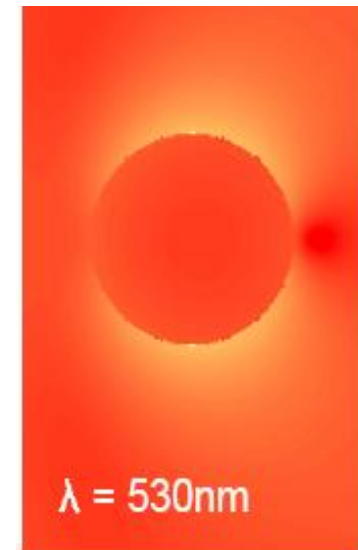
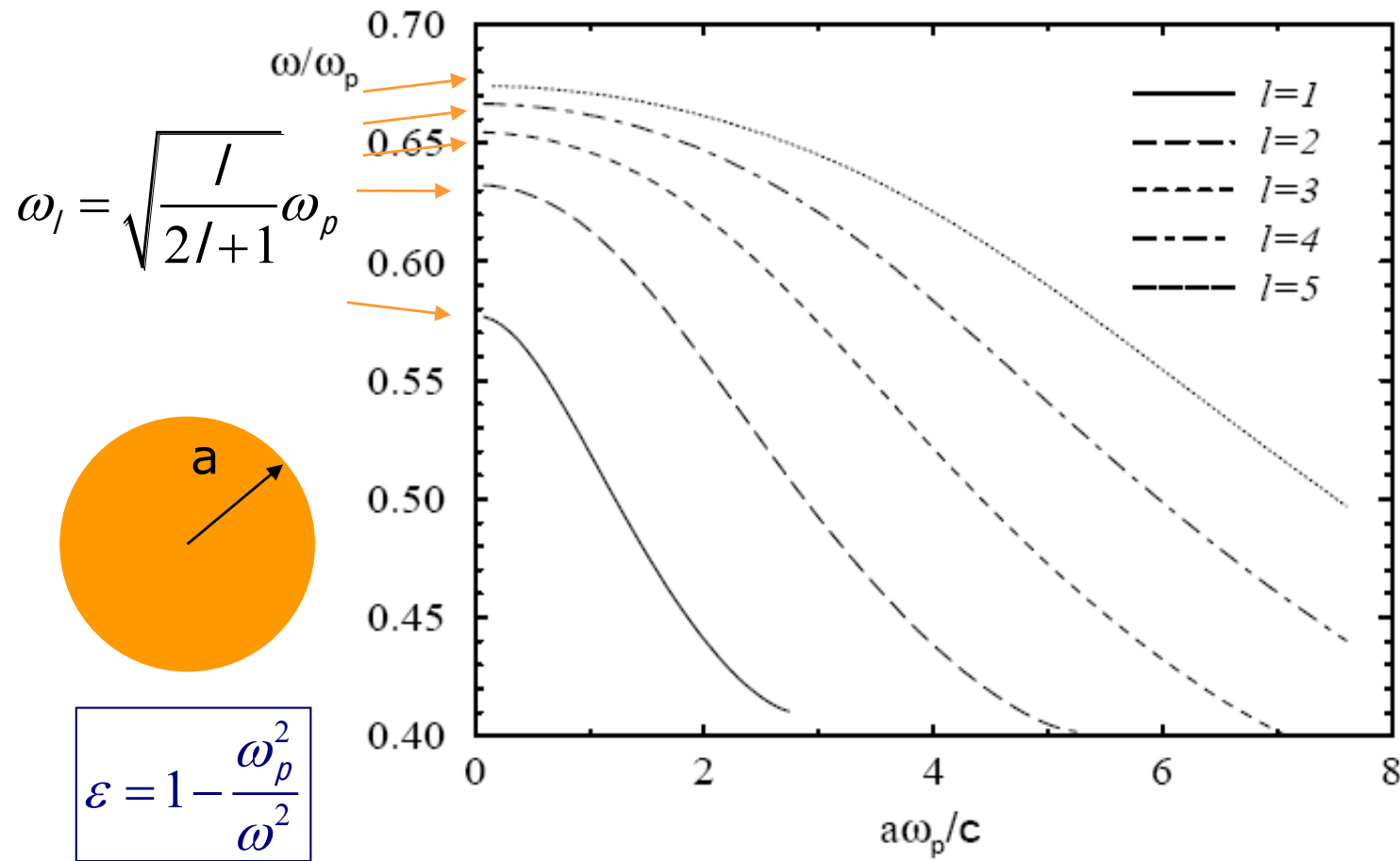


Figure 4.9 Scattering by a sphere with $x = 3$ and $m = 1.33 + i10^{-8}$.

→ **Strong forward scattering**

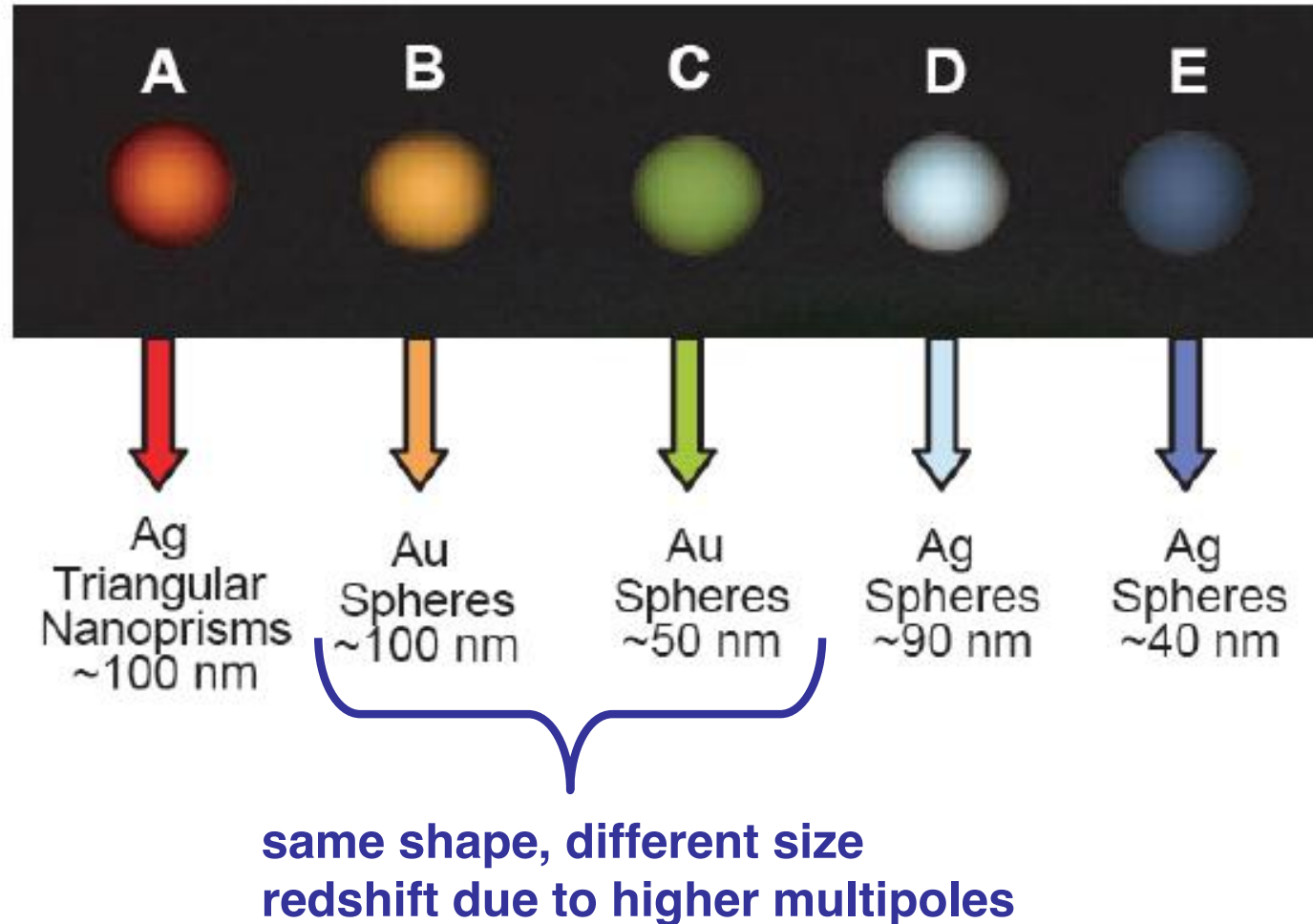
Spherical plasmons: Mie modes derived from Maxwell's equations



l=1 mode

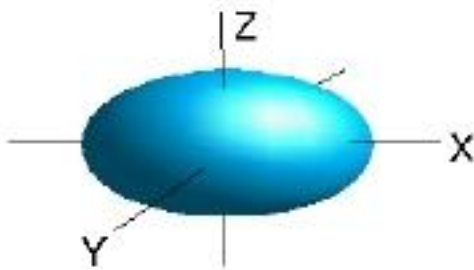
Drude-like metal

Effect of finite size on the resonant frequency



Jin et. al., Science 294, 1901 (2001)

Shape: Polarizability of small ellipsoids



quasistatic approximation:

$$\alpha_{xyz} = \frac{4}{3} \pi abc \frac{\epsilon - \epsilon_m}{\epsilon_m + L_{xyz}(\epsilon - \epsilon_m)}$$

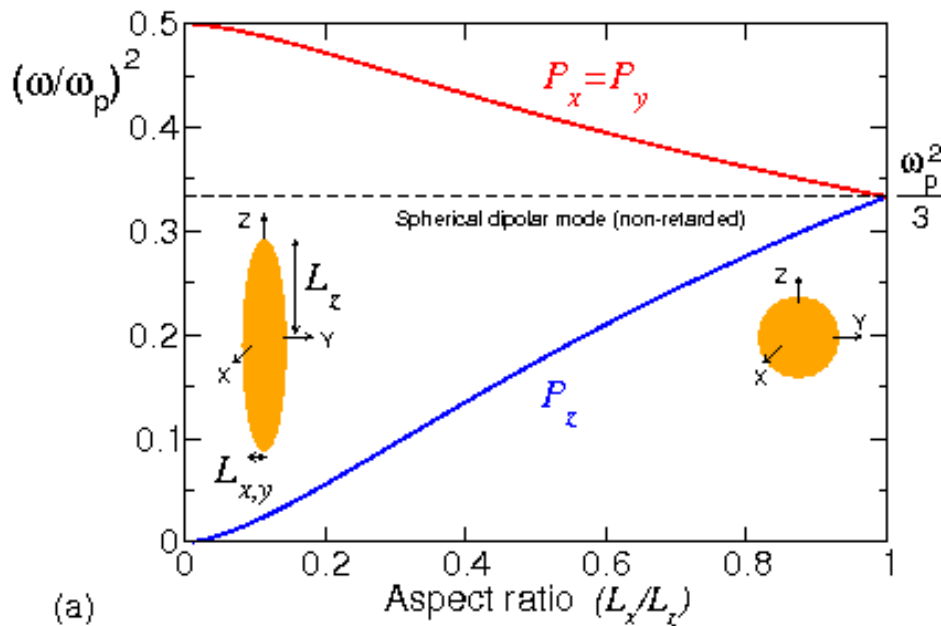


geometrical factors

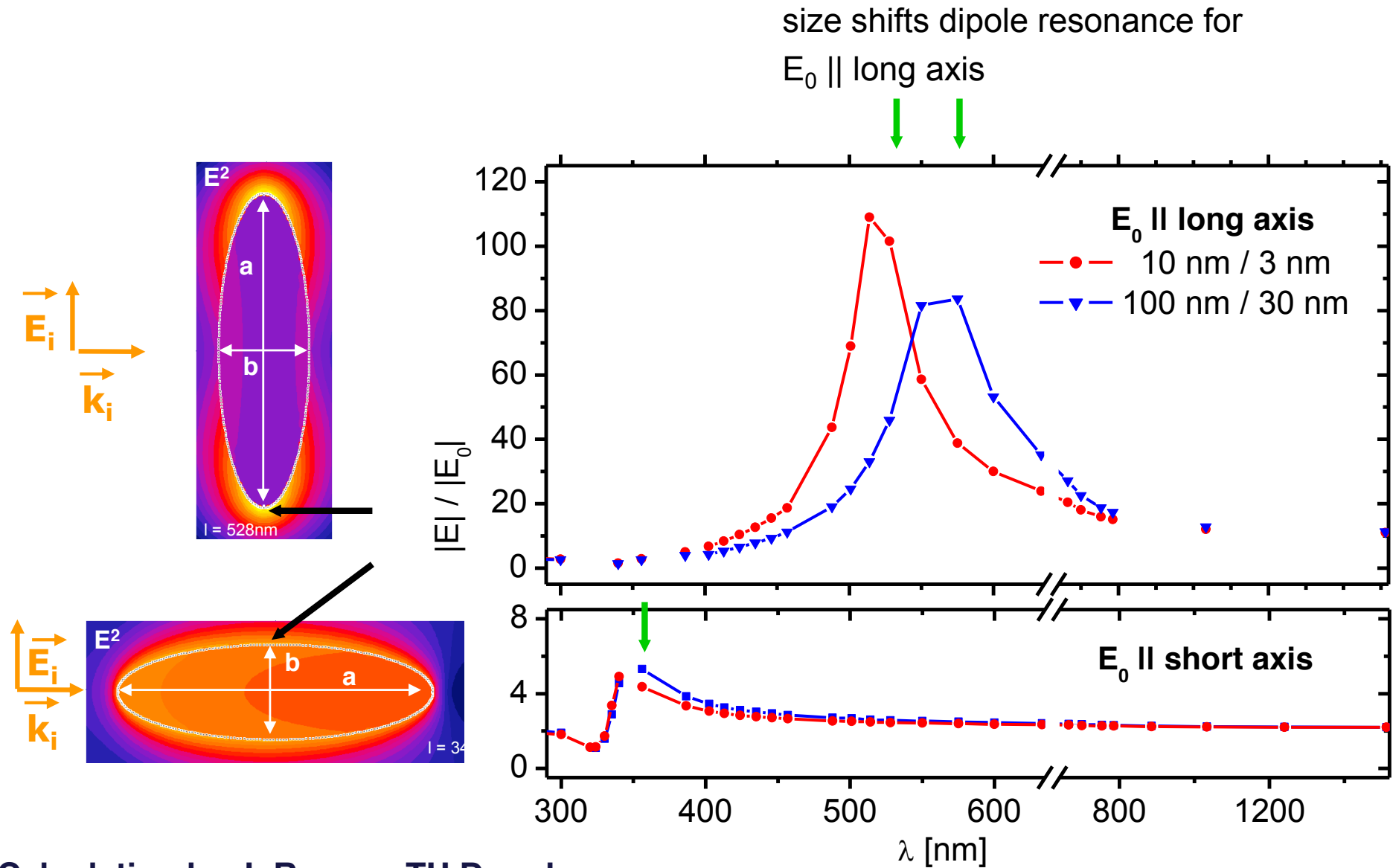
sphere: $L_x = L_y = L_z = \frac{1}{3}$

generally: $L_x \neq L_y \neq L_z$

→ 3 resonances at $\epsilon = \epsilon_m \left(1 - \frac{1}{L_{xyz}} \right)$



Silver ellipsoid illuminated by a plane wave



Calculation by J. Renger, TU Dresden

Plasmon resonances: dependence on the geometry

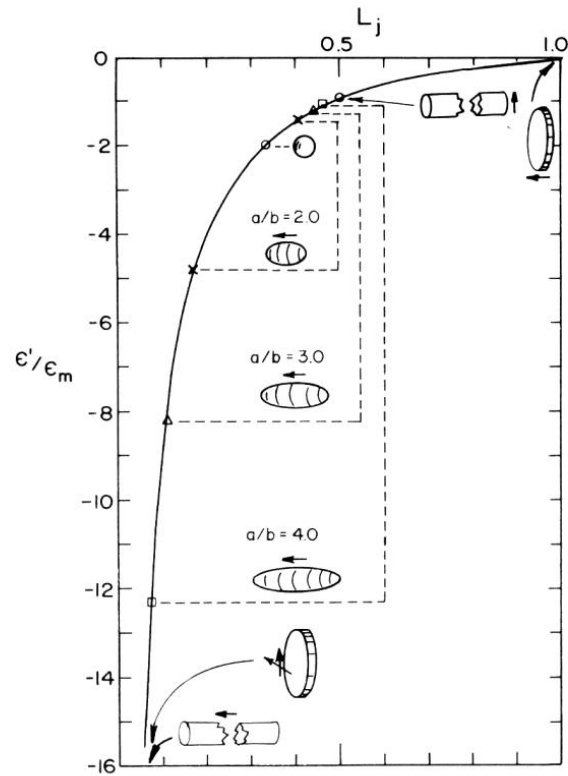


Figure 12.5 Effect of shape on the position of the lowest-order surface mode of small spheroids. Arrows next to the various shapes show the direction of the electric field.

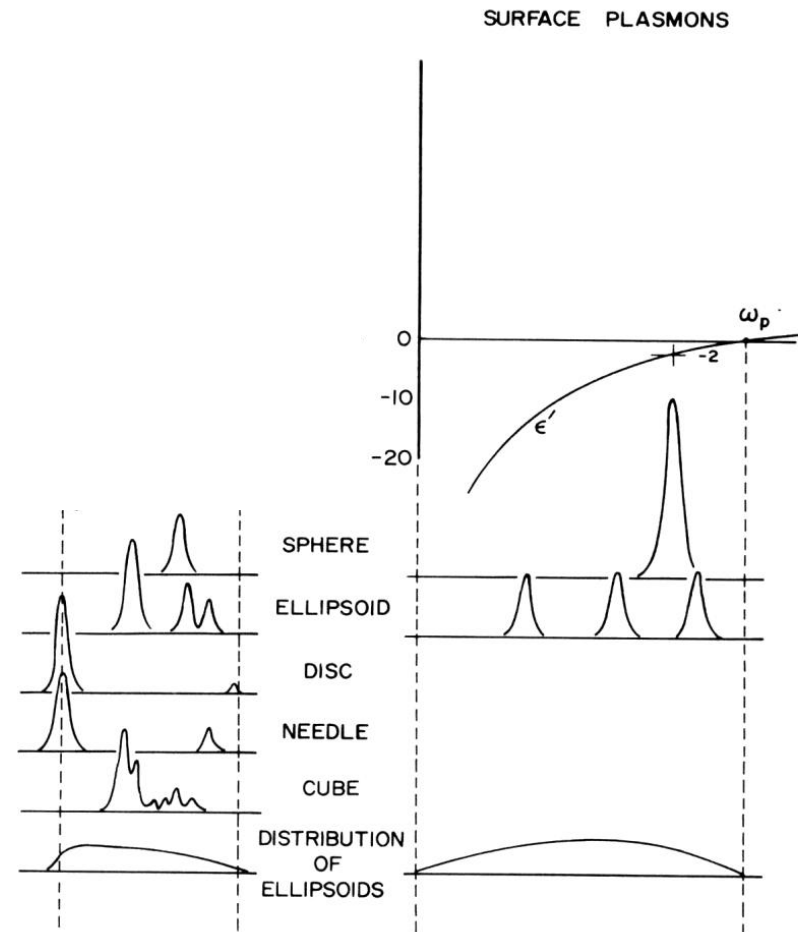
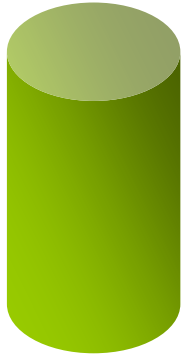


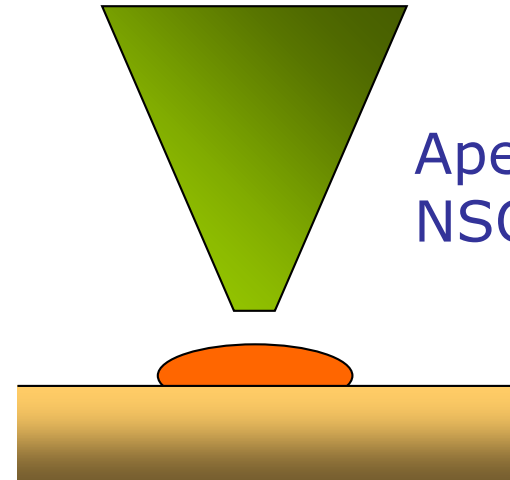
Figure 12.11 Surface mode frequencies for insulating and metallic particles of various shapes.

More complex geometries

Control over the plasmon frequencies by playing with particle **shapes** and **coupling**

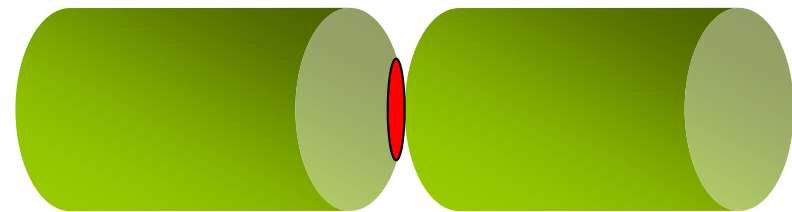
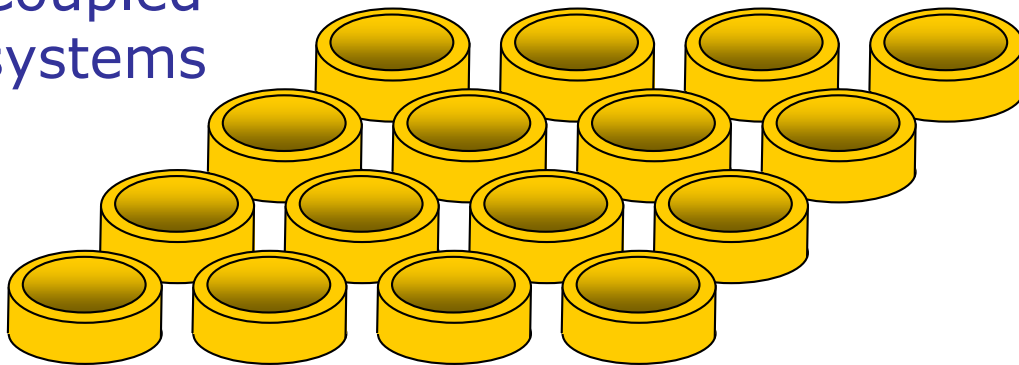


Nanorods, nanoshells,
nanorings, dimers,.....



Apertureless
NSOM

Coupled
systems



Nanometrology, sensing,
spectroscopy

Numerical solutions to the 3D electromagnetic problem

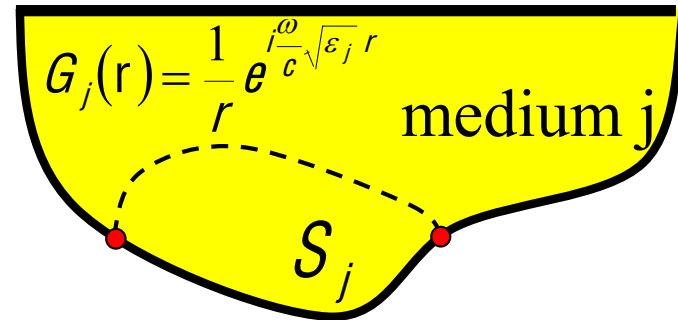
	periodic systems	finite geometries	convergence for high dielectric contrast (e.g., in metals)	effective dimensionality of the problem	
discrete-dipole approximation ▪ Purcell+Pennypacker: optical modes of grains ▪ Martin: Green-function formulation			good	3D	
boundary element method ▪ JGA and Howie			good	2D	
finite difference in the time domain ▪ Joannopoulos photonic crystals			poor	3D	
plane wave expansions ▪ Leung			poor	3D	
transfer matrix approach ▪ Pendry			poor	2D	
multiple scattering ▪ Ohtaka: LEED-like methods to photons ▪ Wang, Stefanou, Sheng: photonic crystals ▪ JGA: finite systems					

Boundary Element Method

$$\mathbf{E}(\mathbf{r}) = i\frac{\omega}{c} \mathbf{A}(\mathbf{r}) - \nabla\phi(\mathbf{r})$$

$$\mathbf{A}(\mathbf{r}) = \mathbf{A}^{\text{ext}}(\mathbf{r}) + \int_{S_j} d\mathbf{s} G_j(\mathbf{r}-\mathbf{s}) \mathbf{h}_j(\mathbf{s})$$

$$\phi(\mathbf{r}) = \phi^{\text{ext}}(\mathbf{r}) + \int_{S_j} d\mathbf{s} G_j(\mathbf{r}-\mathbf{s}) \sigma_j(\mathbf{s})$$



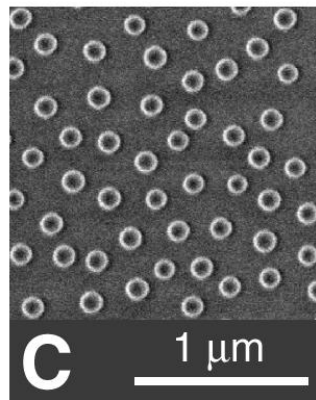
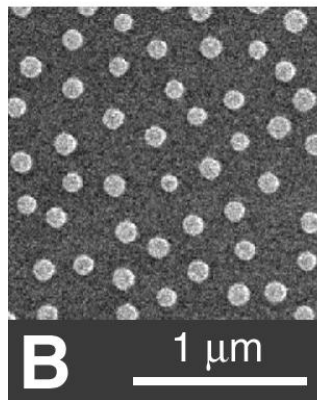
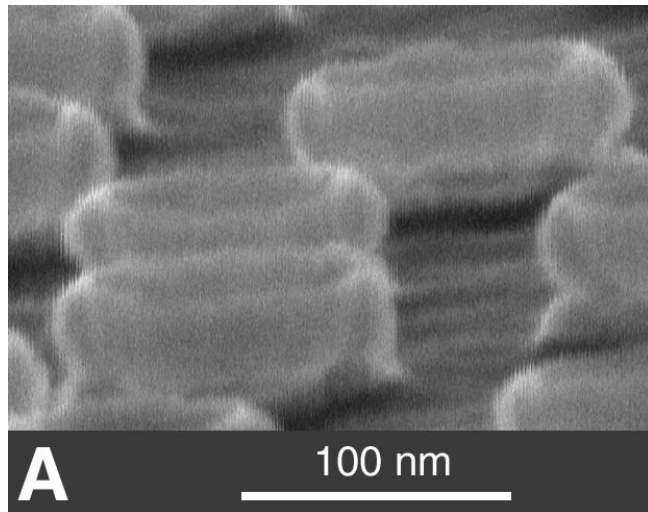
The boundary conditions lead to a set of surface integral equations with the interface currents \mathbf{h}_j and charges σ_j as variables. For example, the continuity of ϕ leads to

$$\int_{S_j} d\mathbf{s}' \left[G_1(\mathbf{s}-\mathbf{s}') \sigma_1(\mathbf{s}') - G_2(\mathbf{s}-\mathbf{s}') \sigma_2(\mathbf{s}') \right] = \phi_2^{\text{ext}}(\mathbf{s}) - \phi_1^{\text{ext}}(\mathbf{s}),$$

(1 and 2 refer to the interface sides). The surface integrals are now discretized using N representative points \mathbf{s}_i . This leads to a system of $8N$ linear equations with $\mathbf{h}_1(\mathbf{s}_i)$, $\mathbf{h}_2(\mathbf{s}_i)$, $\sigma_1(\mathbf{s}_i)$, and $\sigma_2(\mathbf{s}_i)$ as unknowns.

García de Abajo and Aizpurua, PRB **56**, 15873 (1997) García de Abajo and Howie, PRB **65**, 115418 (2002)

An example of Optical Antenna: Optical properties of metallic nanorings

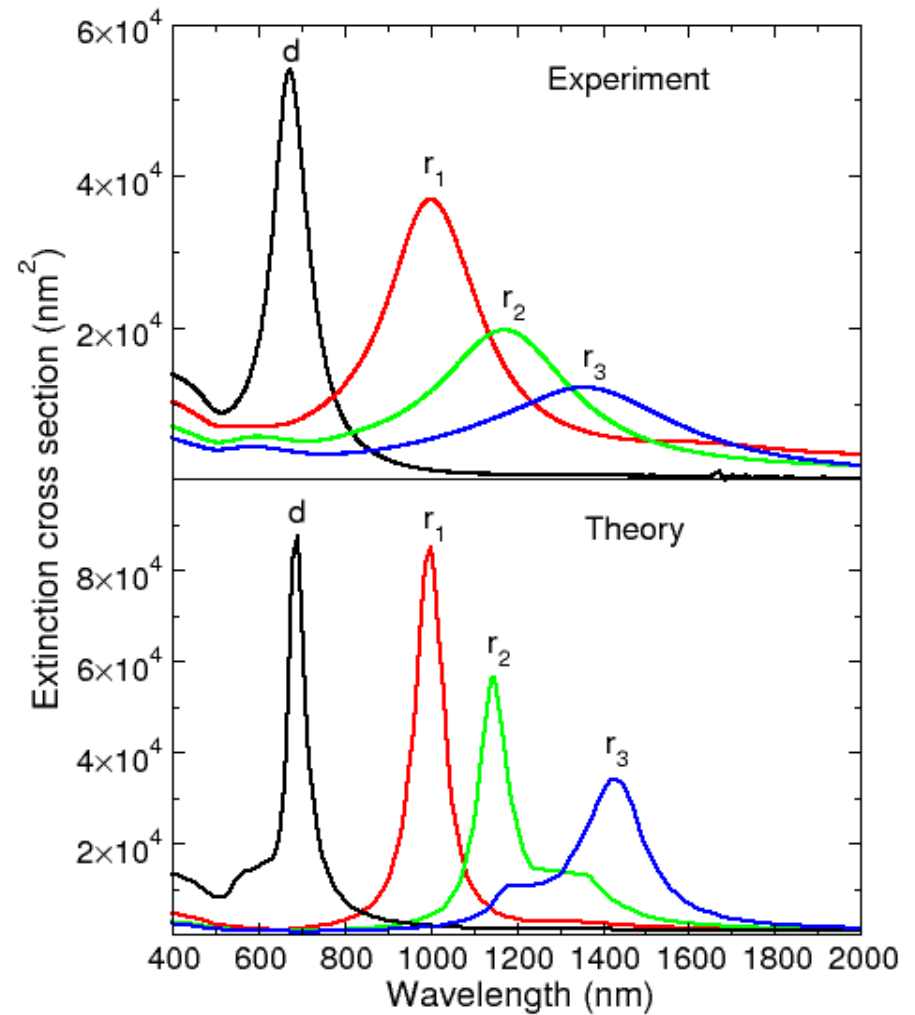


Disk

Nanoring

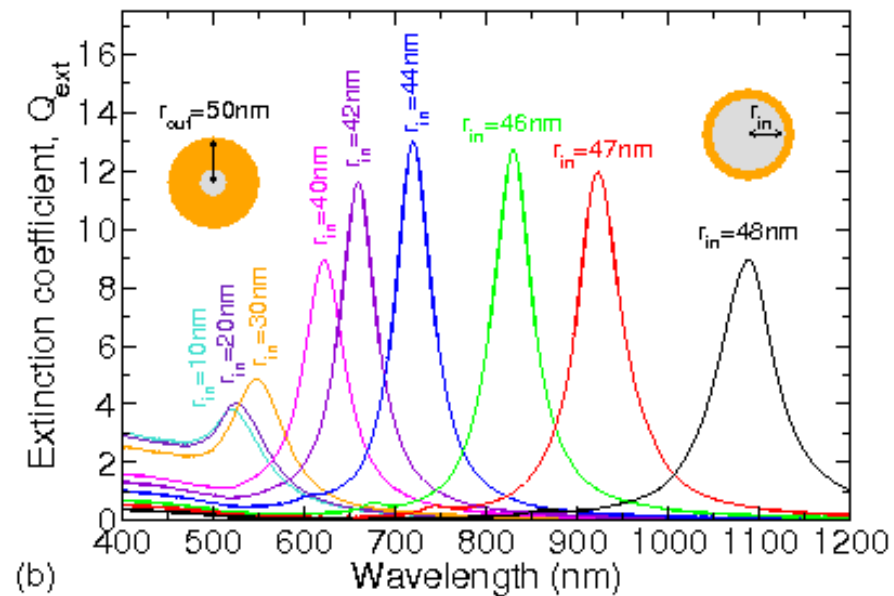
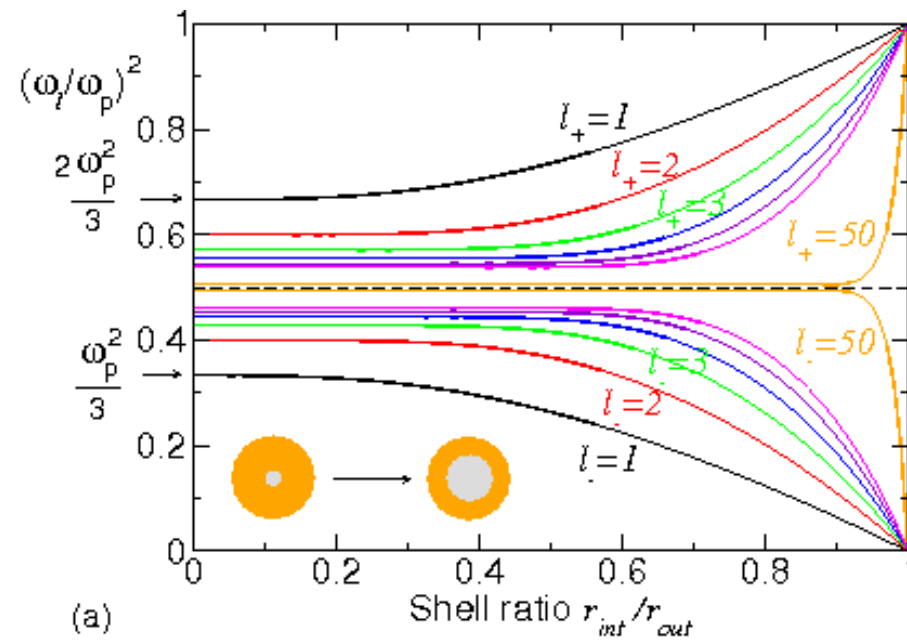


d/a smaller \rightarrow red shift



Aizpurua *et al.* Phys. Rev. Lett. **90**, 057401 (2003)

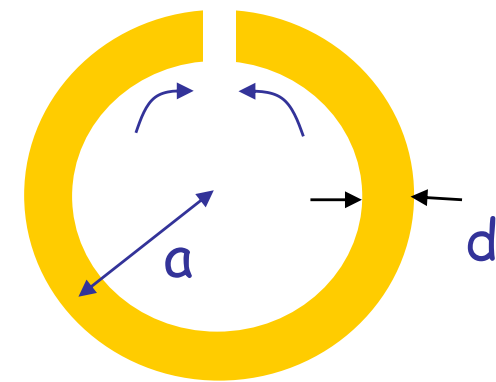
Optical properties of metallic nanoshells



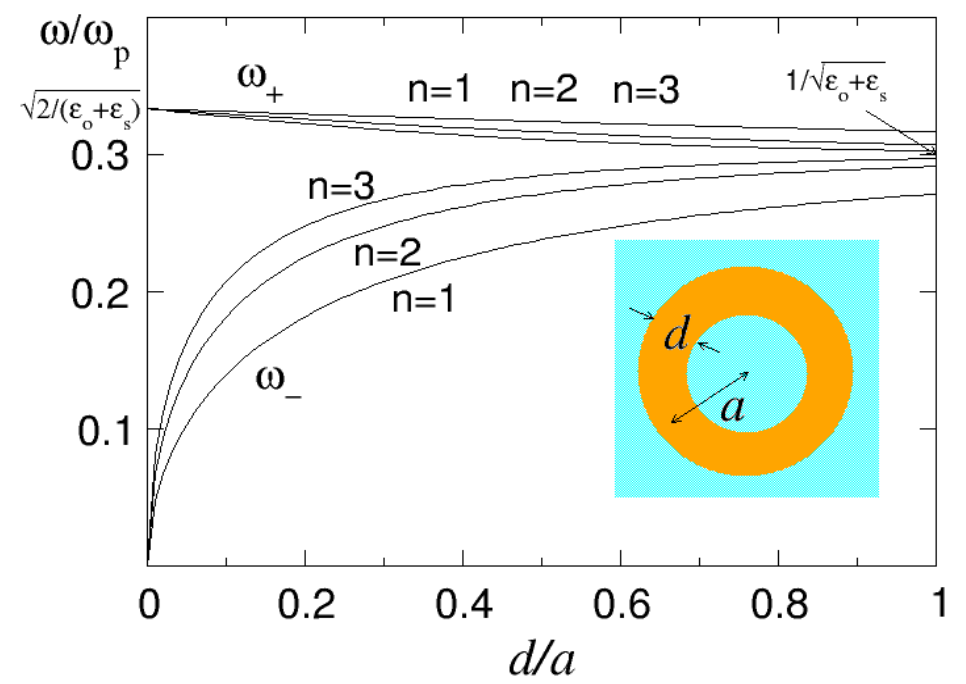
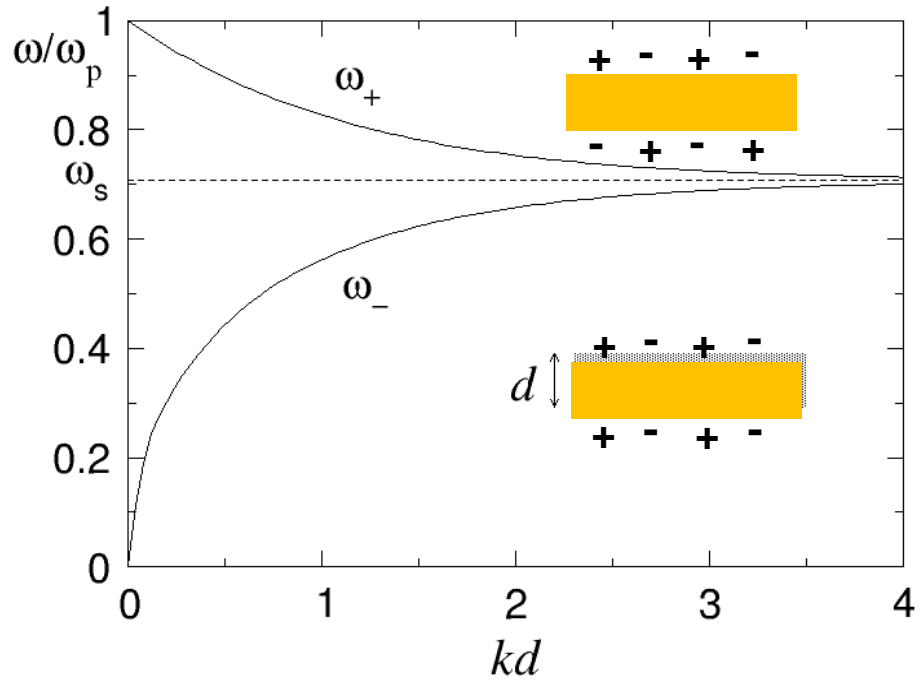
Modes in a nanoring. The twisted slab



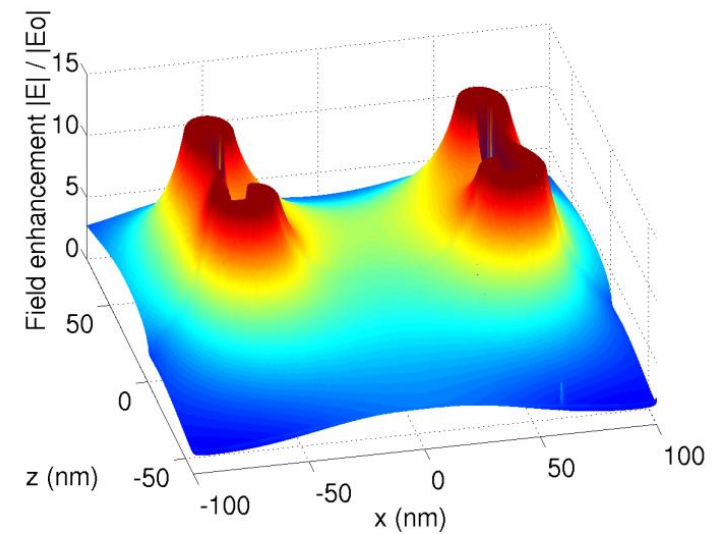
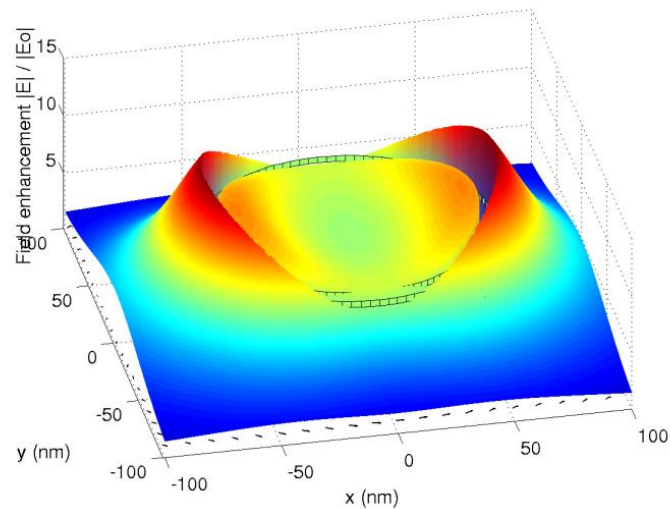
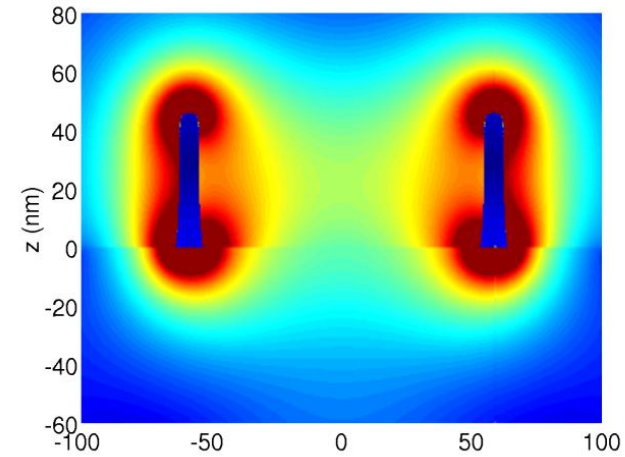
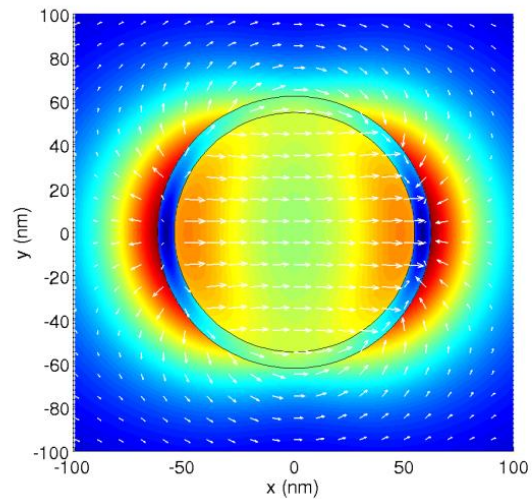
$$\omega_{\pm} = \omega_s (1 \pm e^{-kd})^{1/2}$$



$$kd = n \frac{2\pi}{L} d = n \frac{d}{a}$$



Field-enhancement in a nanoring



Radio Frequency Antennas



Half wave dipole antennas



Biconical antenna



Monopole antenna



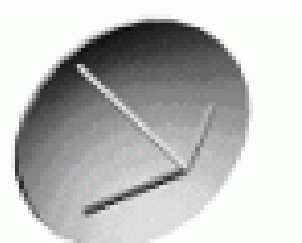
Comilog antenna



Yagi-Uda antenna



Horn antenna

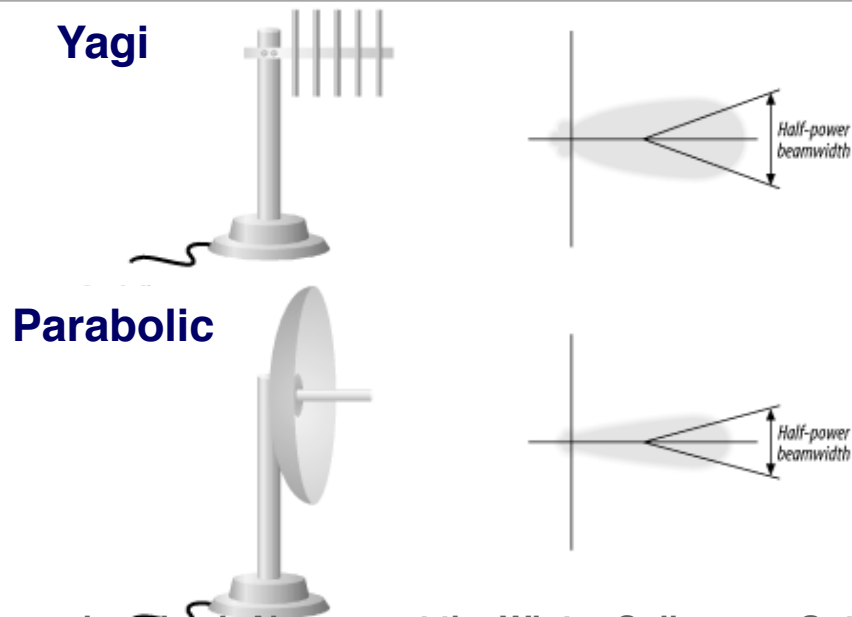
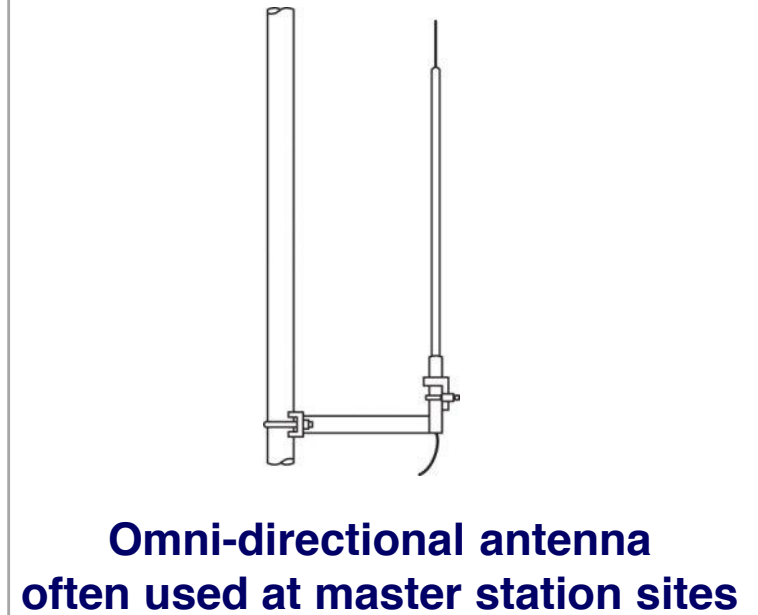
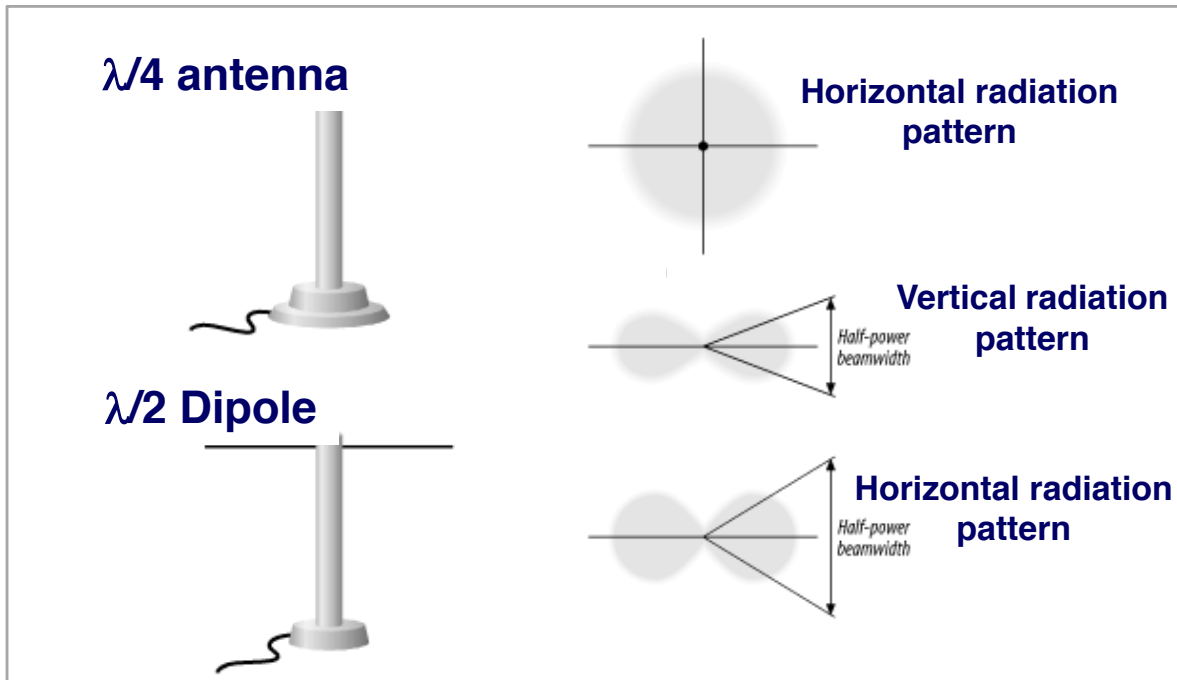


Parabolic antenna

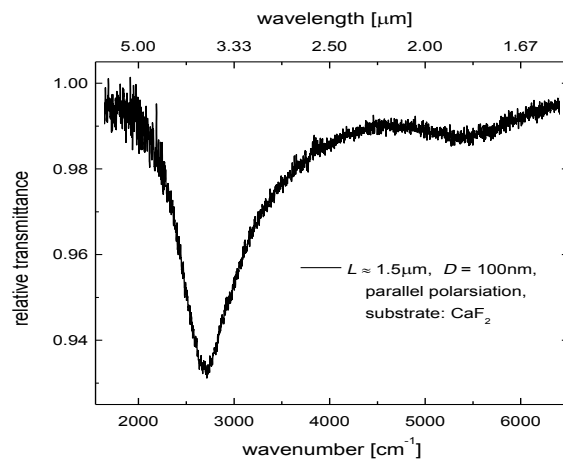
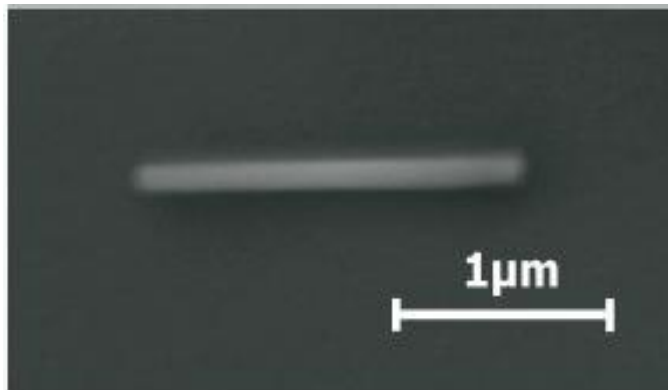


Active loop antenna

Different types of radio antennas

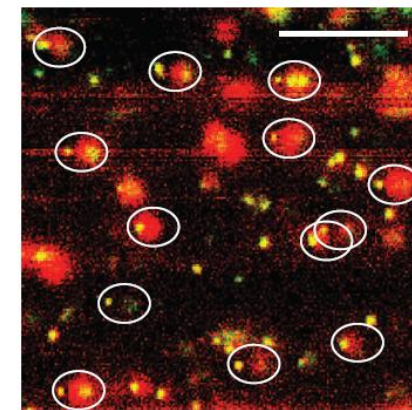
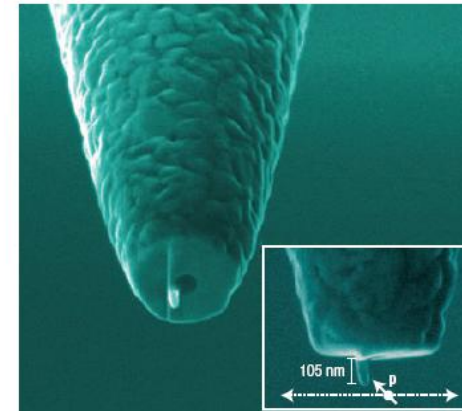


$\lambda/2$ nanoantenna



**Neubrech *et al.*,
App. Phys. Lett. 89, 253104 (2006)**

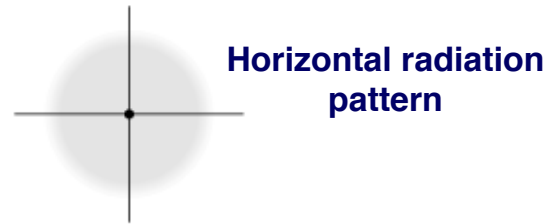
$\lambda/4$ optical antenna



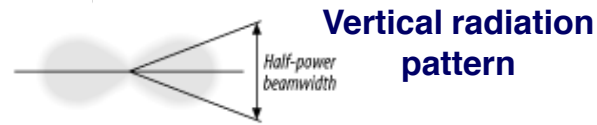
**Taminiau *et al.*,
Nature Photonics 2, 234 (2008)**

Different types of radio antennas

Vertical

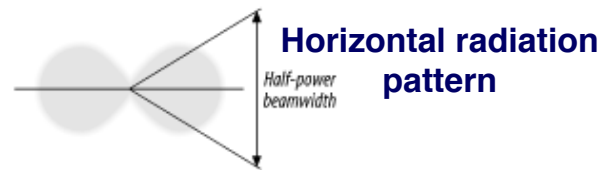


Horizontal radiation pattern

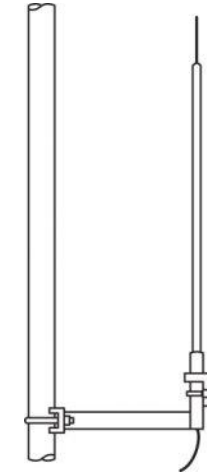


Vertical radiation pattern

Dipole

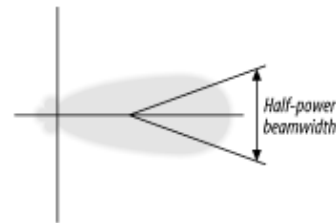


Horizontal radiation pattern

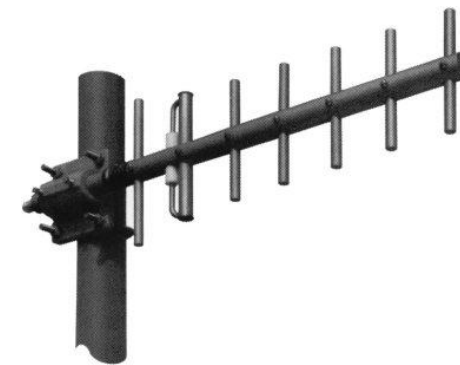


Omni-directional antenna often used at master station sites

Yagi

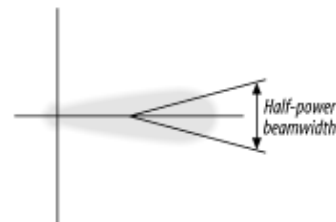


Half-power beamwidth



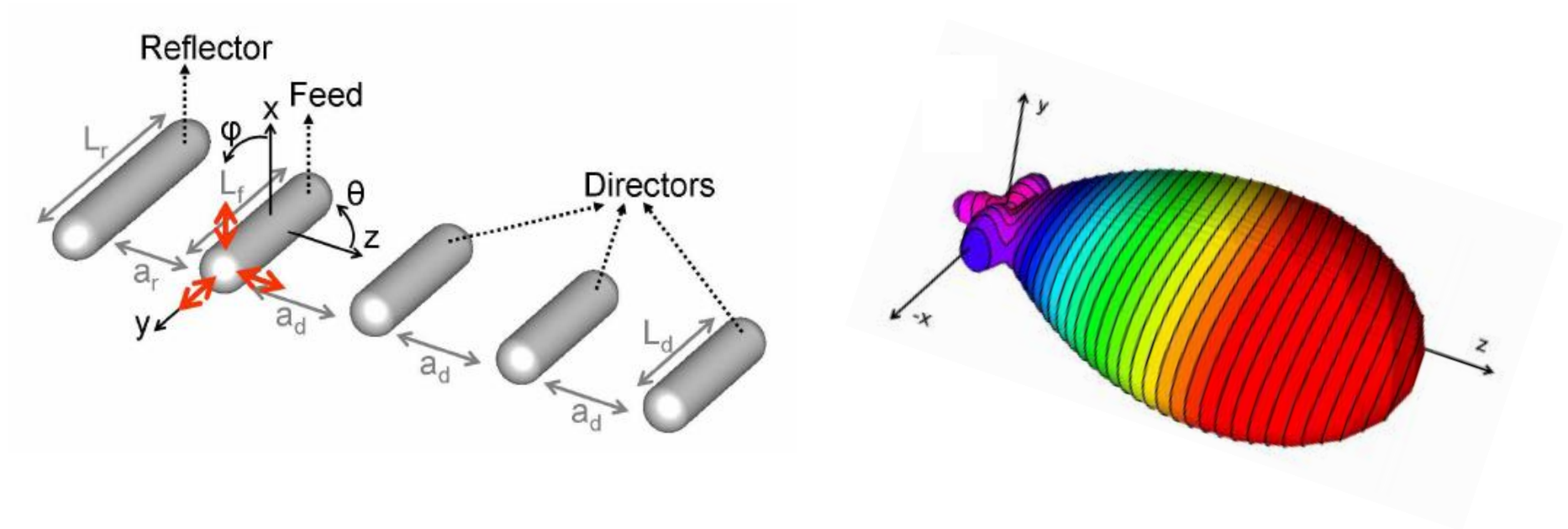
**Directional Yagi antenna
Commonly used at remote field sites**

Parabolic



Half-power beamwidth

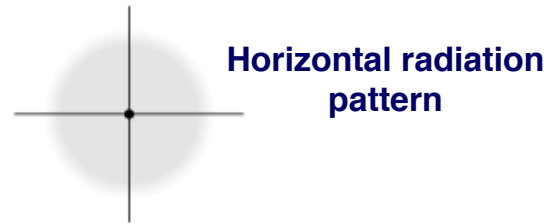
Yagi-Uda antenna



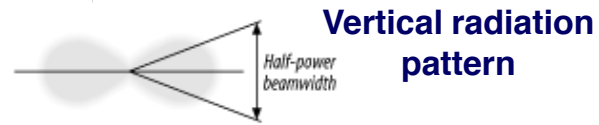
**Taminiau *et al.*,
Optics Express 14, 10858 (2008)**

Different types of radio antennas

Vertical

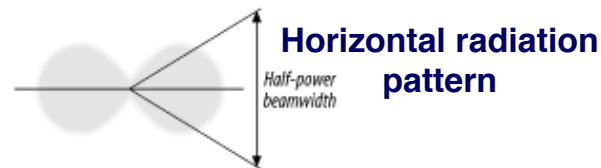


Horizontal radiation pattern



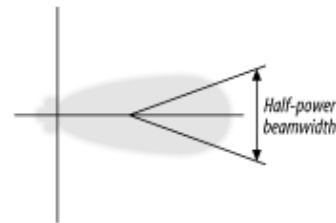
Vertical radiation pattern

Dipole



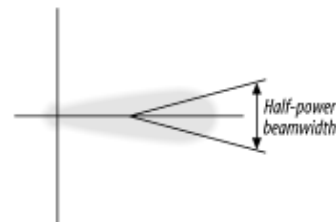
Horizontal radiation pattern

Yagi

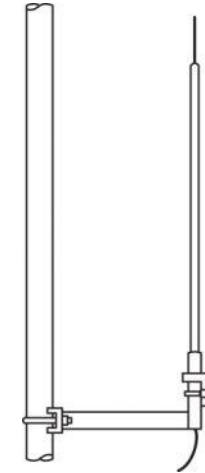


Half-power beamwidth

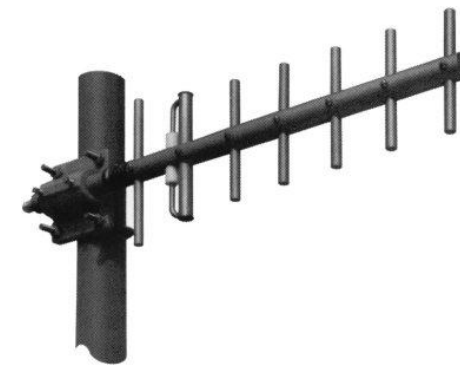
Parabolic



Half-power beamwidth

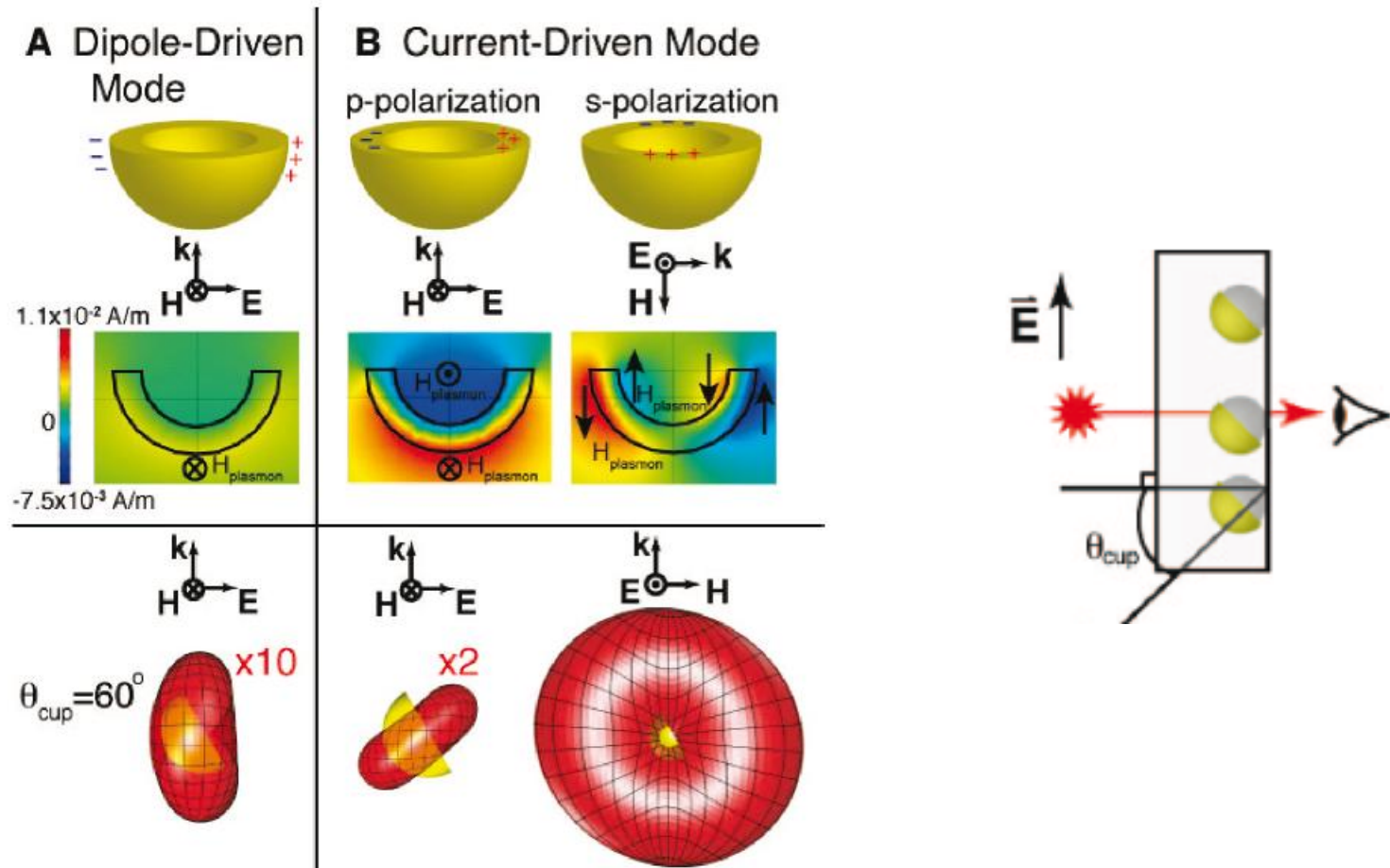


**Omni-directional antenna
often used at master station sites**



**Directional Yagi antenna
Commonly used at remote field sites**

Parabolic-like optical nanoantennas

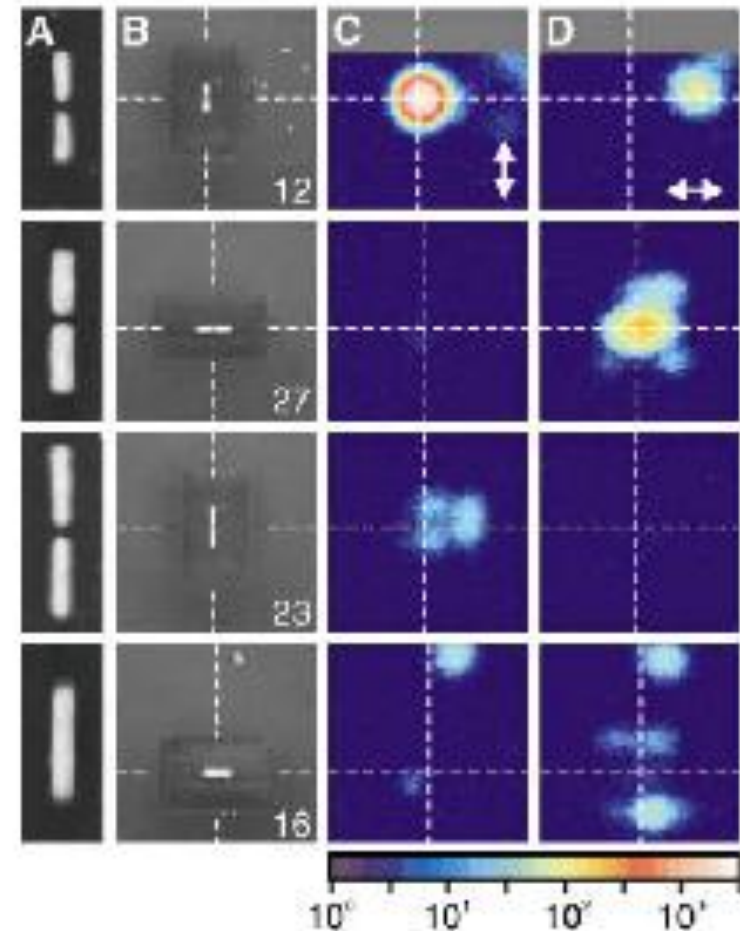
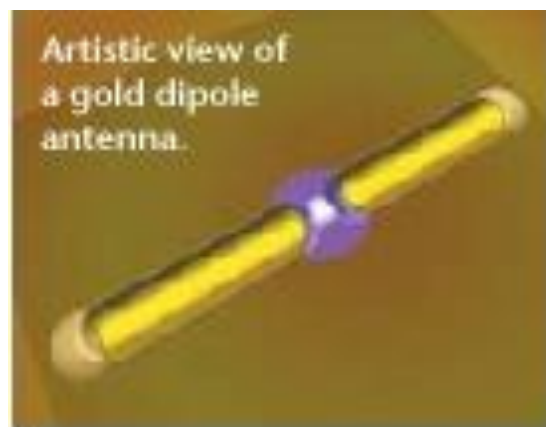
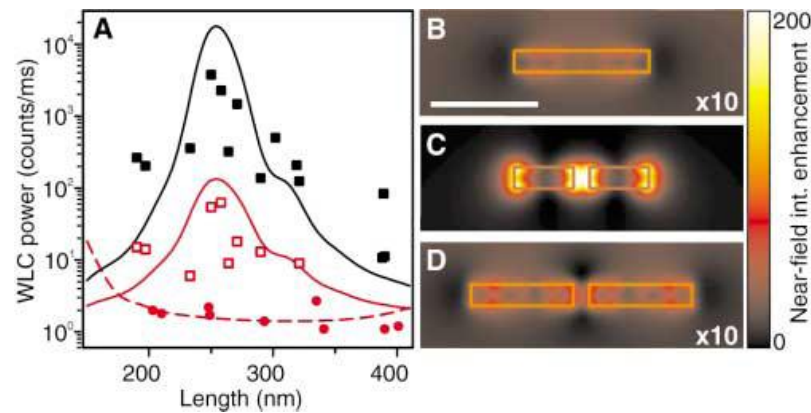


N. Mirin and N. Halas, Nano Letters 9, 1255 (2009)

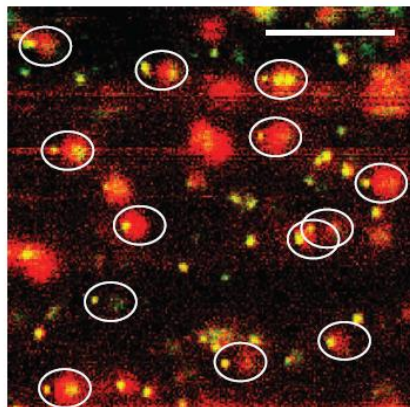
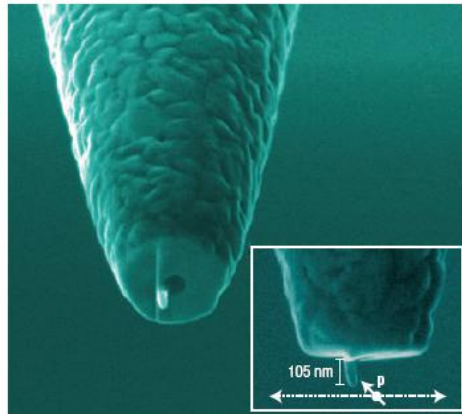
Resonant Optical Antennas

P. Mühlischlegel,¹ H.-J. Eisler,¹ O. J. F. Martin,² B. Hecht,^{1*}
D. W. Pohl¹

SCIENCE VOL 308 10 JUNE 2005

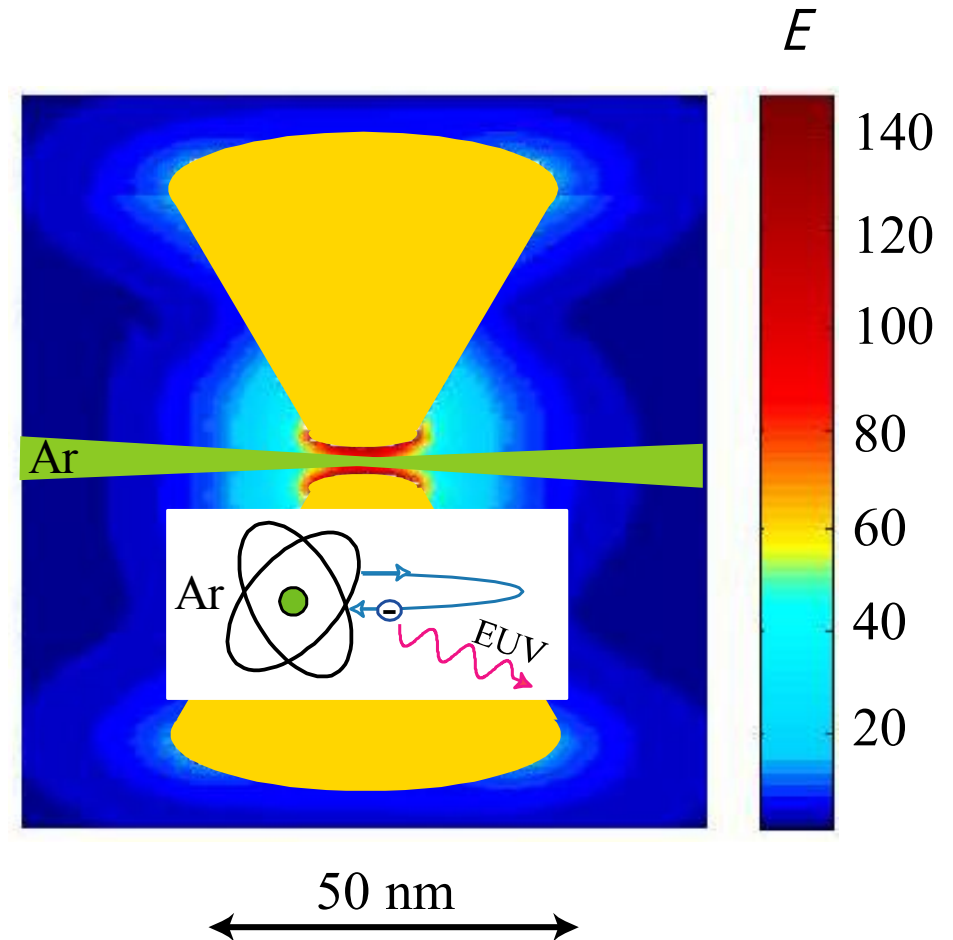


$\lambda/4$ optical antenna



**Taminiau *et al.*,
Nature Photonics 2, 234 (2008)**

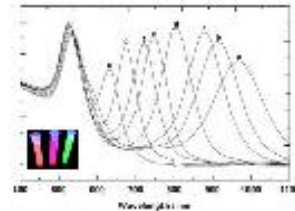
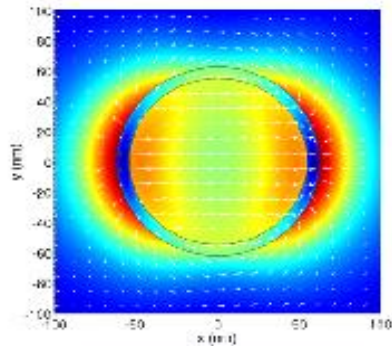
Bowtie antennas



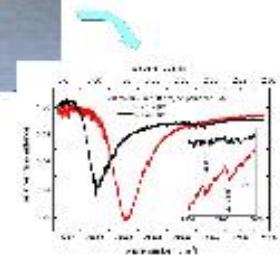
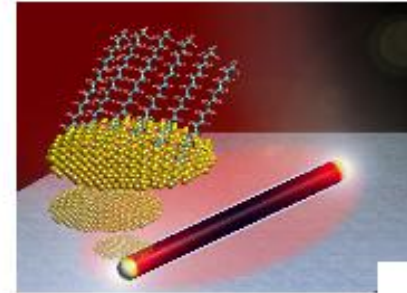
Nature 453, 731 (2008)

Plasmonic antennas

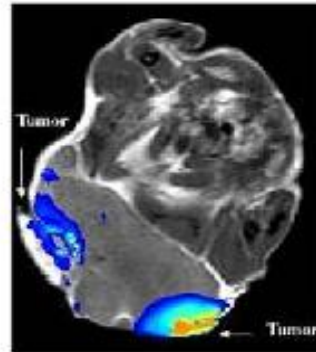
Fundamentals of metallic nano-optical components (optical response)



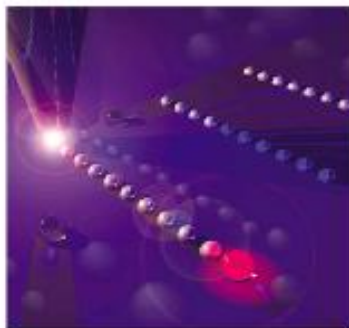
Plasmon-enhanced spectroscopies and microscopies (SERS, SEIRA, s-SNOM)



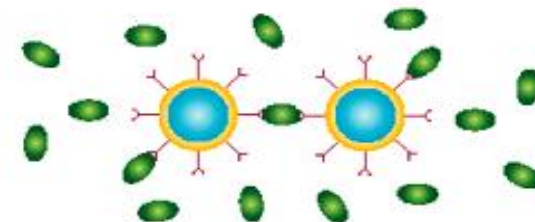
Biomedical applications



Optical guides, interconnects in opto-electronic devices



Sensing and biolabeling



Thank you for your attention!

<http://cfm.ehu.es/nanophotonics>